# The nitrogen phosphotransferase regulator PtsN ($EIIA^{Ntr}$) regulates inorganic polyphosphate production in *Escherichia coli*.

Marvin Q. Bowlin [a,*], Abagail R. Long [a,*], Joshua T. Huffines [a], and Michael J. Gray[a,#]

Department of Microbiology, School of Medicine, University of Alabama at Birmingham, Birmingham, AL 35294 [a]

Running Head: PtsN regulates polyP synthesis

* These authors contributed equally to this work. Author order was determined alphabetically.

[#] Address correspondence to Michael J. Gray, mjgray@uab.edu

## ABSTRACT

Inorganic polyphosphate (polyP) is synthesized by bacteria under stressful environmental conditions and acts by a variety of mechanisms to promote cell survival. While the kinase that synthesizes polyP (PPK, enocoded by the *ppk* gene) is well known, little is understood about how environmental stress signals lead to activation of this enzyme. Previous work has shown that the transcriptional regulators DksA, RpoN ($\sigma^{54}$), and RpoE ($\sigma^{24}$) positively regulate polyP production, but not *ppk* transcription, in *Escherichia coli*. In this work, we set out to examine the role of the alternative sigma factor RpoN and nitrogen starvation stress response pathways in controlling polyP synthesis in more detail. In the course of these experiments, we identified GlnG, GlrR, PhoP, PhoQ, RapZ, and GlmS as proteins that affect polyP production, and uncovered a central role for the nitrogen phosphotransferase regulator PtsN ($EIIA^{Ntr}$) in a polyP regulatory pathway, acting upstream of DksA, downstream of RpoN, and apparently independently of RpoE. However, none of these regulators appears to act directly on PPK, and the mechanism(s) by which they modulate polyP production remain unclear. Unexpectedly, we also found that the pathways that regulate polyP production vary depending not only on the stress condition applied, but also on the composition of the media in which the cells were grown before exposure to polyP-inducing stress. These results constitute substantial progress towards deciphering the regulatory networks driving polyP production under stress, but highlight the remarkable complexity of this regulation and its connections to a broad range of stress-sensing pathways.


## IMPORTANCE

Bacteria respond to changes in their environments with a complex regulatory network that controls the expression and activity of a wide range of effectors important for their survival. This stress response network is critical for the virulence of pathogenic bacteria and for the ability of all bacteria to grow in natural environments. Inorganic polyphosphate (polyP) is an evolutionarily ancient and almost universally conserved stress response effector that plays multiple roles in virulence, stress response, and survival in diverse organisms. This work provides new insights into the connections between well characterized nitrogen starvation and cell envelope stress response signaling pathways and the production of polyP in *Escherichia coli*.

## INTRODUCTION

Inorganic polyphosphate (polyP) is a biopolymer of up to hundreds of phosphate units that is produced by organisms of all domains of life (1-3). In bacteria, polyP has been known to be required for stress response and virulence for decades (4-6), and recent work has begun to decipher molecular mechanisms by which bacterial polyP directly disrupts phagocytic cell functions important in the host immune response to bacterial infections (7-11). These results have led to a growing interest in polyP metabolism and the recent identification of a range of chemicals that inhibit the bacterial polyP kinases (PPKs) responsible for polyP synthesis as promising potential anti-virulence drug candidates (7, 12-15).

Despite this, relatively little is known about how polyP production is regulated in bacteria. In the model organism *Escherichia coli*, polyP is undetectable during

exponential growth in rich medium, but is synthesized rapidly upon exposure to a variety of stress conditions, including severe oxidative stress, heat shock, salt stress, and multiple types of starvation stresses (16-18). Early work identified a few regulators in *E. coli* that affected polyP synthesis under different conditions, but did not establish the mechanisms by which these acted (16, 19, 20). In *E. coli*, PPK and the polyP-degrading enzyme exopolyPase (PPX) are encoded in a bicistronic operon (21) whose transcription does not increase upon stress treatment (17, 22, 23). However, our previous results have shown that transcriptional regulators are required for robust polyP production in response to a nutrient limitation stress in which exponential-phase cultures of *E. coli* are shifted from rich medium into phosphate-limited glucose minimal medium (16). These include the RNA polymerase-binding protein DksA (24) and the stress-responsive alternative sigma factors RpoE and RpoN (22). These observations led us to hypothesize that these transcription factors regulate the expression of genes or proteins responsible for directly activating PPK activity under stress conditions. However, the transcriptional response to nutrient limitation is complex, and transcriptomics have not allowed us to identify any such directly-acting regulators to date (22).

The experiments described in this paper were aimed at deciphering the role of RpoN-dependent genes in polyP regulation. RpoN is the *E. coli* $\sigma^{54}$-family sigma factor, and is notable for requiring additional ATPase proteins for activation of transcription at specific promoters (25, 26). These bacterial enhancer binding proteins (bEBPs) control specific and well-defined regulons in *E. coli* (27), and we hypothesized that by determining

which bEBP(s) were necessary for polyP production we would be able to identify specific RpoN-dependent polyP regulators.

In the course of testing this hypothesis, we discovered that the bEBP GlnG, involved in the classical nitrogen starvation response in *E. coli* (28), is a positive regulator of polyP synthesis, but that this activity and the effect of RpoN on polyP synthesis are suppressed by the presence of glutamine in the rich medium before nutrient limitation, growth conditions under which polyP is not being produced. Further studies revealed that glutamine had a significant effect on which regulatory pathways were required for polyP synthesis after nutrient limitation, and that this was true not only of RpoN and GlnG, but also of RapZ, a regulator of the peptidoglycan precursor synthesis enzyme GlmS (29). The cell envelope stress responsive regulators GlrR (30-32) and PhoP (33) both also impacted polyP production, acting as negative regulators. By examining known nitrogen-responsive regulatory systems in *E. coli*, we identified a key role for the nitrogen phosphotransferase regulator PtsN ($EIIA^{Ntr}$) (34) as an activator of polyP synthesis that acts downstream of RpoN, upstream of DksA, and apparently independently of RpoE.

The results of these studies are new insights into the network of regulators involved in modulating polyP production in *E. coli* and an increased appreciation that media composition can impact not only the extent of polyP synthesis but also the regulators involved in controlling that synthesis. However, all of the regulators we have identified

so far appear to act indirectly, and we have yet to identify the genes, proteins, or metabolites directly responsible for activation of PPK under stress conditions.

## RESULTS

**The bEBPs GlnG and GlrR influence polyP production.** As we have previously reported (22), Δ*rpoN* mutant *E. coli* had a significant defect in polyP synthesis upon nutrient limitation stress (Fig. 1A). Expression of *rpoN* from a plasmid rescued this phenotype, but did not increase polyP production in a wild-type strain (Fig. 1A). RpoN-dependent promoters require bEBPs (25, 26), so to narrow down the identity of the RpoN-dependent gene(s) involved in polyP synthesis, we measured polyP production in mutants lacking each of the 11 bEBPs present in *E. coli* MG1655 (27) (Figs. 1B,C). Mutants lacking *glnG* (also known as *ntrC*)(28) had a significant defect in polyP production and mutants lacking *glrR* produced significantly more polyP than the wild-type (Fig. 1B). These phenotypes canceled each other out, and a Δ*glrR* Δ*glnG* double mutant produced an amount of polyP indistinguishable from the wild-type. No other bEBP mutations affected the extent of polyP synthesis under these conditions (Fig. 1C).

**RpoN-dependent regulation of polyP synthesis is dependent on cellular nitrogen status, but not on GlnB or GlnK *per se*.** The involvement of GlnG in polyP synthesis implicates the cellular response to nitrogen starvation in polyP regulation (28), which was not unexpected based on previous reports in the literature (16, 35). Under nitrogen limitation conditions, perceived by the cell as a decrease in the ratio of intracellular glutamine to glutamate and an accumulation of α-ketoglutarate (28, 36, 37), glutamine

synthase (GlnA) is activated by a pathway involving the PII signaling proteins GlnB and GlnK (28, 38-41)(Fig. 2A). Transcription of *glnB* is constitutive, but *glnK* transcription is activated by RpoN and GlnG (28, 41, 42) (Fig. 2B), and *glnK* induction is a reliable reporter of cellular nitrogen starvation (41). Consistent with our previously-reported RNA sequencing data (22), polyP-inducing nutrient limitation strongly induced *glnK* expression (Fig. 2C). The gene encoding *glrR* is immediately adjacent to *glnB* in the *E. coli* genome, and the Δ*glrR* mutation used here deletes not only most of the coding sequence of that gene (43), but also deletes a binding site for the repressor PurR in the *glnB* promoter region (44, 45) (Fig. 2B). We therefore hypothesized that GlnK or GlnB, which regulate the activity of a variety of proteins by direct interaction (28, 38, 46-48), might be activators of polyP synthesis. To test this idea, we expressed *glnB* and *glnK* from arabinose-inducible plasmids, but found that neither *glnB* nor *glnK* overexpression increased polyP production in wild-type, Δ*rpoN*, or Δ*dksA* mutant strains (Figs. 2D,E). Mutants lacking both *glnB* and *glnK* are glutamine auxotrophs (49), and LB, the rich medium used for the “before stress” growth condition (16), is naturally very low in glutamine (50), so we tested whether Δ*glnB*, Δ*glnK*, or Δ*glnBK* mutations affected polyP production after nutrient shift from rich media supplemented with glutamine (LBQ; Fig. 2F). There was a very slight defect in polyP production in the Δ*glnB* mutant, but the more surprising result was that, although the extent of polyP production after shift from LBQ into minimal medium was very similar to that after shift from LB (Figs. 2D,E,F), neither *rpoN* nor *glnG* mutants had any defect in polyP synthesis under these conditions. This was unexpected and showed that cellular nitrogen status affects the regulatory pathway by which polyP synthesis is activated. This observation probably

150 also explains the very high variability in polyP production we have previously reported in
151 a Δ*glnG* mutant (24) in experiments performed with a different supply of LB medium.
152 This was not true for the Δ*dksA* mutant (22, 24), which was defective in polyP synthesis
153 regardless of whether the LB was supplemented with glutamine (Fig. 2F). Glutamine
154 concentration is a common signal of cellular nitrogen status sensed by many regulators
155 and enzymes (28, 37), so we tested whether PPK itself was allosterically regulated by
156 either glutamate or glutamine, and found that neither of these compounds affected the
157 activity of purified PPK *in vitro* at physiological concentrations (51) (Fig. 2G).
158
159 **Effect of *glmY* and GlmS (glutamine--fructose-6-phosphate aminotransferase)**
160 **regulation on polyP production.** Since we could not attribute the effect of the Δ*glrR*
161 mutation on polyP synthesis (Fig. 1B) to disregulation of *glnB* (Fig. 2D), we examined
162 the possible role of the GlrR regulon on polyP synthesis. GlrR is activated by GlrK, a
163 histidine kinase that responds to cell envelope disruptions (30). In *E. coli* MG1655, GlrR
164 is only known to regulate the expression of two promoters, that of the operon encoding
165 the alternative sigma factor RpoE and that of the sRNA *glmY* (31, 32) (Fig. 3A). We
166 have previously reported that Δ*rpoE* mutants have significant defects in polyP synthesis,
167 indicating that RpoE is a positive regulator of polyP production (22). Regulation of the
168 *rpoE* operon is complex (32, 52, 53), but GlrR is an activator of *rpoE* expression (32), so
169 it is difficult to reconcile a model in which this explains the increase in polyP production
170 in the Δ*glrR* mutant (Fig. 1B). We therefore turned our attention to *glmY*, which, in a
171 pathway involving the RNA-binding protein RapZ and the sRNA *glmZ*, is responsible for
172 increasing GlmS (glutamine--fructose-6-phosphate aminotransferase) synthesis under

conditions where intracellular glucosamine-6-phosphate (GlcN6P) becomes limiting (29, 31, 54)(Fig. 3A). GlcN6P, synthesized by GlmS from glutamine and fructose-6-phosphate, is an essential precursor of the peptidoglycan cell wall (55, 56), and so is linked to both cell envelope stress and cellular nitrogen status. Deletion of *phoP* or *phoQ*, encoding a two-component regulator that responds to environmental stresses, including low pH and magnesium limitation, and is known to also positively regulate *glmY* (33), also led to a significant increase in polyP synthesis (Fig. 3B), consistent with this being the mechanism by which the Δ*glrR* mutation does so (Fig. 1B). PhoP is a global regulator that affects the expression and stability of many proteins (33), but is best known for its role in activating magnesium import (33, 57). High levels of polyP synthesis can cause magnesium starvation in *E. coli*, presumably by chelating the metal (23). However, deletion of the PhoP-regulated magnesium stress response genes *mgtA* and *mgtS* had no effect on polyP synthesis (Fig. 3B), and polyP-inducing nutrient shift did not activate the magnesium starvation response (Supplemental Fig. S1). PolyP-inducing nutrient limitation conditions did strongly downregulate *glmS* expression (Fig. 3C). Neither fructose-6-phosphate nor GlcN6P affected the activity of PPK *in vitro* (Fig. 3D).

**PolyP regulation by RapZ and GlmS depends on growth conditions.** Given the phenotypes of the Δ*glrR* and Δ*phoP* mutants (Figs. 1B, 3B), we hypothesized that deletion of *glmY* would increase the amount of polyP produced by *E. coli* and that either deletion of *rapZ* or *glmZ* or overexpression of *glmS* would decrease polyP production (Fig. 3A). However, under our normal nutrient limitation conditions, none of these had

any effect on polyP synthesis (Figs. 4A,B). We wondered whether this was due to inadequate expression of *glmS* from an arabinose-inducible promoter in minimal medium containing glucose (58), so performed a nutrient shift into minimal medium containing arabinose as a sole carbon source (Fig. 4C). Under these conditions, polyP accumulation in the vector-only control was approximately half of that seen after nutrient shift into glucose, but *glmS* expression did significantly reduce polyP production. Nutrient shift from glutamine-supplemented rich medium into minimal glucose medium also resulted in modest, but statistically significant, defects in polyP synthesis in a Δ*rapZ* mutant and upon *glmS* overexpression (Figs. 4D,E). Nutrient shift from LB into minimal medium with glucosamine as a sole carbon source, expected to result in very high levels of intracellular glucosamine and low GlmS activity (59-61), resulted in significantly less polyP production than shift into glucose, and shift into glycerol, expected to result in low intracellular glucosamine and therefore high GlmS activity (51, 60) resulted in no detectable polyP production at all (Fig. 4F). The extent of polyP production was not affected by supplementation of the rich medium with glucosamine (Supplemental Fig. S2). These results reinforce the observation that growth conditions impact not only the extent of polyP synthesis, but the pathways involved in its regulation, and indicate that regulators of GlmS can, under certain circumstances, impact polyP production, with a general correspondence between higher polyP levels when GlmS levels are low and *vice versa*, but can not fully explain the mechanism by which this occurs.

**PtsN positively regulates polyP synthesis regardless of its phosphorylation state or the presence of glutamine, but does not do so by interacting directly with PPK.**

The nitrogen phosphotransferase system ($PTS^{Ntr}$) is a regulatory cascade that responds to nitrogen limitation and regulates the activity of multiple proteins in *Enterobacteriacea*, including both GlmS and PhoP (62-67)(Fig. 5A). The genes encoding PtsN (also known as $EIIA^{Ntr}$) and NPr, homologs of the EIIA and HPr proteins of the well-characterized carbon PTS (68), are encoded in the *rpoN* operon (34). PtsP (also known as $EI^{Ntr}$), which is homologous to EI of the carbon PTS (34, 68), responds to both glutamine and α-ketoglutarate as signals of cellular nitrogen limitation by autophosphorylation (37, 69), ultimately resulting in phosphorylation of NPr and PtsN (70). Both NPr and PtsN interact with and regulate the activity of a variety of proteins, typically depending on their phosphorylation states (62-67). Based on these facts and our results showing roles for PhoP and GlmS in polyP regulation we hypothesized that the $PTS^{NTr}$ might form part of the link between nitrogen limitation and polyP synthesis.

Mutants lacking *ptsN* were defective in polyP synthesis (Fig. 5B). However, this defect was not affected by glutamine supplementation and was not seen in Δ*npr* or Δ*ptsP* mutants (Figs. 5B,C), suggesting that phosphorylation was not important for this phenotype. Indeed, both the non-phosphorylatable $PtsN^{H73A}$ variant and the phosphorylated form-mimicking $PtsN^{H73E}$ variant (71, 72) complemented the polyP defect of a Δ*ptsN* mutant as well as did wild-type PtsN (Fig. 5D). PtsN regulates other proteins by direct physical interaction (62-67), so we used a bacterial two-hybrid assay (73) to test whether PtsN interacts with PPK *in vivo*, and found that it does not (Fig. 5E). PPK activity is also not affected by α-ketoglutarate *in vitro* (Fig. 5F), eliminating this metabolite as a possible allosteric regulator of polyP production.

**Effect of polyP-inducing nutrient limitation on PtsN levels *in vivo*.** The only reported example of a protein in *Enterobacteria* that interacts with both the phosphorylated and dephosphorylated forms of PtsN is PhoP (33, 62). In *Salmonella*, PtsN inhibits PhoP binding to DNA, and in turn, PhoP regulates the proteolytic degradation of PtsN, leading to a decrease in PtsN protein concentration under PhoP-activating conditions (Fig. 5A). Both abundance and phosphorylation of PtsN are therefore potential variables in any PtsN-dependent regulatory system. PtsN abundance in *Salmonella* is also regulated in response to carbon source availability (63). We constructed strains encoding chromosomal fusions of the 3xFLAG epitope tag to the C-terminus of PtsN (62) to allow us to determine whether our polyP-inducing stress conditions led to changes in PtsN abundance in *E. coli*. In wild-type and Δ*phoP* strains (Figs. 6A,B), there was no significant change in PtsN abundance after nutrient limitation, consistent with the apparent lack of PhoP induction under these conditions (Supplemental Fig. S1). There was a significant increase in PtsN abundance two hours after nutrient limitation in a Δ*rpoN* mutant (Fig. 6C), but this increase did not correlate with polyP accumulation, which is lower in this strain (Fig. 1A). Based on these results, the regulation of polyP by PtsN does not appear to depend on PtsN abundance.

**PtsN acts downstream of RpoN, upstream of DksA, and independently of RpoE in polyP regulation.** Finally, we used complementation analysis to examine the relationships between the different regulators of polyP production we have identified. PtsN, RpoN, DksA, and RpoE are all positive regulators of polyP production (Figs. 1,

5)(22, 24). Expressing RpoN from a plasmid does not increase polyP synthesis in a Δ*ptsN* mutant (Fig. 7A), but expressing either DksA or RpoE does (Fig. 7B). In contrast, expressing PtsN rescues polyP production in Δ*rpoN* and Δ*rpoE* mutants, but not in a Δ*dksA* mutant (Figs. 7C,D,E). This suggests a pathway in which, in response to nutrient limitation stress, RpoN positively regulates PtsN, which in turn positively regulates DksA, increasing polyP production. We do not, at this time, know which of these activation steps are direct and which are indirect or the mechanism by which DksA activates polyP production (22, 24). The case of RpoE is more complicated. Since the defects of Δ*rpoE* and Δ*ptsN* mutants can each be rescued by expression of the other gene (Figs. 7B,E), the simplest interpretation is that they regulate polyP production by independent mechanisms. However, *ptsN* is both a member of the RpoE regulon (74) and a multicopy suppressor of the conditionally lethal phenotype of a Δ*rpoE* mutant (75), so these results must be interpreted cautiously. Expression of RpoN rescues the polyP defect of a Δ*rpoE* mutant (22), DksA is a positive regulator of RpoE-dependent transcription for some genes (76), and there are known interactions between RpoN and RpoE in response to combined nitrogen and carbon starvation stress conditions (77). We think it is unlikely, therefore, that these regulators are operating completely independently in control of polyP production, but do not yet have enough data to speculate on their exact relationship.

## DISCUSSION

It is perhaps unsurprising that the regulation of polyP synthesis is complex, given the ancient evolutionary roots of polyP (3, 6, 78, 79) and the intricacy of the regulatory

288 networks for other general stress response pathways in bacteria. In *E. coli*, for example,
289 there are at least 20 regulators of the stress-responsive sigma factor RpoS known at
290 time of writing, acting at the transcriptional, post-transcriptional, and post-translational
291 levels (27, 80, 81). Envelope stress responses are equally complex and involve a
292 variety of interacting and overlapping pathways and regulons, the details of which are
293 still not fully understood (53, 82).
294
295 The experiments presented in this paper were intended to identify the gene or genes
296 regulated by RpoN that contribute to polyP production (16, 22), and while we did
297 successfully identify roles for the RpoN-related proteins GlnG, GlrR, and PtsN in
298 modulating polyP production (Figs. 1, 5), we did not find a simple RpoN-dependent
299 activator of polyP production and uncovered unexpected impacts of PhoPQ, RapZ, and
300 GlmS (Figs. 3, 4). Some of these regulators only impacted polyP production under
301 specific growth conditions. Adding glutamine to the rich media before nutrient limitation
302 makes RpoN and GlnG unneccessary for polyP production (Fig. 2F), but makes RapZ
303 and GlmS expression significant regulators (Fig. 4D,E). The carbon source in the
304 minimal medium also affects both polyP production and the impact of GlmS expression
305 on that production (Fig. 4C,F). Based on this, one important conclusion we can draw
306 from our results is that, while shift from rich medium to minimal medium is in general a
307 strong signal inducing polyP production (16, 24), the composition of both the rich and
308 minimal media impacts not only the extent of polyP production, but also the pathways
309 involved in regulating that production. This is not, in hindsight, completely surprising, but
310 does mean that growth in LB medium (50) can not simply be considered a “non-stress”

311 condition that contrasts with “stressful” nutrient limitation, and that in order to fully
312 understand polyP regulation we will also need to consider the cell’s physiological state
313 under conditions when it is not producing detectable amounts of polyP.
314
315 The exact function of the PTS$^{Ntr}$ has been debated for some time (28, 34), but it is clear
316 from our results that PtsN has a phosphorylation-independent positive effect on polyP
317 synthesis (Figs. 5, 7). What is less clear is how this occurs. PtsN does not appear to
318 interact directly with PPK *in vivo* (Fig. 5E). Overexpression of PtsN is known to
319 generally reduce cell envelope stress in *E. coli*, although the mechanism by which it
320 does so is not well understood (75). Known targets of PtsN regulation include proteins
321 involved in phosphate transport (83), potassium transport (84-86), GlcN6P synthesis
322 (64), and environmental sensing (62). While phosphate transport is certainly important
323 for polyP synthesis (16, 19, 87, 88) and PtsN-dependent changes in potassium levels
324 are known to impact sigma factor specificity (85), which may also play a role in polyP
325 regulation (22), both of these phenotypes are dependent on the phosphorylation state of
326 PtsN, as is the interaction between PtsN and GlmS (64). While this manuscript was in
327 preparation, Gravina *et al*. (89) reported the identification of multiple new PtsN
328 interaction candidates in *E. coli*, most of which also appear to be phosphorylation-state
329 specific. Fortuitiously, we have already tested many of these for potential roles in polyP
330 accumulation (22), including proteins involved in flagellar motility and glycerol
331 metabolism, and found that those pathways have minimal effects on polyP
332 accumulation. However, there are additional candidates, including proteins of unknown

function (*e.g.* YeaG, YcgR, and YcjN) and enzymes of central metabolism (*e.g.* AceAB, PpsA, SucC), that remain to be tested.

Nevertheless, with the information in hand, we identified the interaction between PtsN and the transcription factor PhoP (62) as the most likely candidate for a phosphorylation-independent mechanism for PtsN's effect on polyP accumulation. PhoP is a global regulator that responds to magnesium limitation, low pH, antimicrobial peptides, hyperosmotic stress, periplasmic redox state, and other environmental conditions (33). PtsN inhibits PhoP's DNA binding affinity, thereby potentially impacting transcription of the PhoP regulon and of genes controlled by regulators that are part of that regulon (*e.g.* RstA, MgrR,or IraM)(33, 62, 90). However, PhoP also has large-scale post-translational effects on the proteome by regulating the activity of proteases (33, 91, 92), and PtsN is degraded by the Lon protease under PhoP-activating conditions in a PhoP-dependent feedback loop (62). While PtsN abundance was not regulated in response to nutrient limitation in wild-type or Δ*phoP* strains (Figs. 6A,B), PtsN abundance did increase at late time points in a Δ*rpoN* mutant (Fig. 6C). It is tempting to speculate that this mutant was upregulating PtsN in an attempt to compensate for the loss of RpoN (Fig. 7C), but additional experiments will be needed to test this hypothesis. The increase in polyP production in *phoPQ* mutants (Fig. 3B) is consistent with the hypothesis that PtsN acts in concert with PhoP to regulate polyP production, but it is also possible that there is another PtsN interaction partner involved. Which member(s) of the PhoP regulon besides PtsN might affect polyP production is also unknown.

356 It is important to note that none of the regulators we identified in this paper are
357 absolutely required for induction of polyP synthesis after stress. Some impact polyP
358 production positively (PtsN, GlnG) and some negatively (GlrR, PhoPQ), but every
359 mutant we tested was still able to respond to nutrient limitation stress by increasing
360 polyP production to some extent. This probably indicates that there are redundant
361 mechanisms by which stress signals impact PPK and PPX activity. We know this to be
362 the case for PPX, which is inhibited by both (p)ppGpp and hypochlorous acid-driven
363 oxidation (17, 20). The mechanism(s) by which PPK activity is controlled remain
364 unknown, although the stress-responsive accumulation of polyP in Δ*ppx* mutant strains
365 indicates that such a mechanism must exist (17, 24). Our *in vitro* results (Figs. 2G, 3D,
366 5F) do show that PPK itself is not allosterically regulated by a set of common
367 metabolites whose levels change under nitrogen limitation conditions (28, 37).
368
369 What is clear from our results (Figs. 1, 3, 4, 5) is that multiple pathways that influence
370 cell envelope stress or synthesis impact polyP synthesis in *E. coli*. Without knowing the
371 mechanism by which PPK activity itself is modulated, it is difficult to determine whether
372 these pathways directly regulate polyP synthesis or, alternatively, whether polyP
373 synthesis responds to the changes in cell envelope homeostasis that result from
374 disruption of those regulatory networks (28-30, 32, 33). Based on the data in this and
375 our previous papers (17, 22-24), on balance, we favor the second hypothesis, but are
376 working to clarify this question. PPK is a peripheral membrane protein (93), so it is not
377 impossible that PPK itself is sensitive to changes in the cytoplasmic membrane *in vivo*.
378 If this is the case, it will be difficult to recapitulate PPK regulation *in vitro*. Regardless,

379 our results illustrate previously unknown connections among a variety of well-conserved
380 environmental stress response pathways and show that even as well-studied an
381 organism as *E. coli* still has plenty of capacity to surprise us and confound our
382 expectations.
383

384 ## MATERIALS AND METHODS

385 ### Bacterial strains, growth conditions, and molecular methods

386 All strains and plasmids used in this study are listed in Table 1. We carried out DNA
387 manipulations by standard methods (94, 95) in the *E. coli* cloning strain DH5α
388 (Invitrogen) and grew *E. coli* at 37°C in Lysogeny Broth (LB)(96) containing 5 g $l^{-1}$ NaCl
389 and, where indicated, 5 mM *L*-glutamine (LBQ) or 4 g $l^{-1}$ glucosamine (LBGlcN). We
390 prepared fresh glutamine and glucosamine stock solutions each day. We added
391 antibiotics when appropriate: ampicillin (100 μg $ml^{-1}$), chloramphenicol (17 or 35 μg $ml^{-1}$), gentamycin (30 μg $ml^{-1}$), kanamycin (25 or 50 μg $ml^{-1}$), or spectinomycin (50 μg $ml^{-1}$).
393 We constructed, maintained, and tested all *rpoE* mutant strains in media containing 10
394 μg $ml^{-1}$ erythromycin (97).
395

396 ### Databases and primer design

397 We obtained information about *E. coli* genes, proteins, and regulatory networks from the
398 Integrated Microbial Genomes database (98), EcoCyc (27), and RegulonDB (45). We
399 designed PCR and sequencing primers with Web Primer (www.candidagenome.org/cgi-
400 bin/compute/web-primer) or SnapGene version 5.3.2 (Insightful Science), and
401 mutagenic primers with PrimerX (www.bioinformatics.org/primerx/index.htm). We

designed all primers used for qPCR with Primer Quest (www.idtdna.com; parameter set "qPCR 2 primers intercalating dyes" for qRT-PCR primer design) and confirmed specificity and amplification efficiencies for each primer pair of close to 1. These primers are listed in Table 2.

**Strain construction**

Unless otherwise indicated, all *E. coli* strains were derivatives of wild-type strain MG1655 ($F^-$, *rph-1 ilvG*$^-$ *rfb-50*)(99), and we confirmed all chromosomal mutations by PCR.

We used P1*vir* transduction (24, 100) to move gene knockout alleles from the Keio collection (43) into MG1655, generating strains MJG1480 (Δ*phoP790*::*kan*$^+$), MJG1483 (Δ*mgtA789*::*kan*$^+$), MJG1484 (Δ*phoQ789*::*kan*$^+$), MJG1955 (Δ*glrR728*::*kan*$^+$), MJG1956 (Δ*atoC774*::*kan*$^+$), MJG1969 (Δ*hyfR739*::*kan*$^+$), MJG1970 (Δ*pspF739*::*kan*$^+$), MJG1971 (Δ*norR784*::*kan*$^+$), MJG1972 (Δ*ygeV720*::*kan*$^+$), MJG1973 (Δ*rtcR755*::*kan*$^+$), MJG1974 (Δ*prpR772*::*kan*$^+$), MJG1975 (Δ*zraR775*::*kan*$^+$), MJG1976 (Δ*fhlA735*::*kan*$^+$), MJG2058 (Δ*glnB727*::*kan*$^+$), MJG2061 (Δ*glnK736*::*kan*$^+$), MJG2064 (Δ*glnG730*::*kan*$^+$), MJG2086 (Δ*ptsN732*::*kan*$^+$), MJG2090 (Δ*npr-734*::*kan*$^+$), MJG2091 (Δ*ptsP753*::*kan*$^+$), and MJG2112 (Δ*rapZ733*::*kan*$^+$). We resolved the insertions (101) in MJG1480, MJG1955, MJG2058, MJG2086, and MJG2112 to give strains MJG1501 (Δ*phoP790*), MJG2065 (Δ*glrR728*), MJG2082 (Δ*glnB727*), MJG2089 (Δ*ptsN732*), and MJG2114 (Δ*rapZ733*), then transduced MJG2065 and MJG2082 with Δ*glnG730*::*kan*$^+$ and Δ*glnK736*::*kan*$^+$, respectively, to yield strains MJG2068 (Δ*glrR728* Δ*glnG730*::*kan*$^+$) and MJG2083

425 (Δ*glnB727* Δ*glnK736*::*kan*$^{+}$). Strains lacking both *glnB* and *glnK* are glutamine
426 auxotrophs (39) and were constructed and maintained on LBQ.
427
428 We replaced the *mgtS*, *glmZ,* and *glmY* genes of strain MG1655 with pKD3-derived
429 chloramphenicol resistance cassettes by recombineering (101), using primers 5' AAT
430 TAA GGT AAG CGA GGA AAC ACA CCA CAC CAT AAA CGG AGG CAA ATA ATG
431 GTG TAG GCT GGA GCT GCT TC 3' and 5' ACA CAA CTG TAA CAA GGG GCC
432 GGT TAG GTG AGG GAT TAT CTC CGT TCA TTA CAT ATG AAT ATC CTC CTT AG
433 3', 5' AAG TGT TAA GGG ATG TTA TTT CCC GAT TCT CTG TGG CAT AAT AAA
434 CGA GTA GTG TAG GCT GGA GCT GCT TC 3' and 5' CTT CCT GAT ACA TAA AAA
435 AAC GCC TGC TCT TAT TAC GGA GCA GGC GTT AAA CAT ATG AAT ATC CTC
436 CTT AG 3', or 5' TTA CCA AAC TAT TTT CTT TAT TGG CAC AGT TAC TGC ATA
437 ATA GTA ACC AGT GTG TAG GCT GGA GCT GCT TC 3' and 5' TCG TCA GAC GCG
438 AAT AGC CTG ATG CTA ACC GAG GGG AAG TTC AGA TAC AAC CAT ATG AAT
439 ATC CTC CTT AG 3', to yield strains MJG1479 (Δ*mgtS1000*::*cat*$^{+}$), MJG2151
440 (Δ*glmZ1000*::*cat*$^{+}$), and MJG2155 (Δ*glmY1000*::*cat*$^{+}$).
441
442 We fused a 3xFLAG tag to the C-terminus of the chromosomal *ptsN* gene by
443 recombineering (102). We amplified the 3xFLAG sequence and kanamycin resistance
444 cassette from plasmid pSUB11 (102) with primers 5' GAA GAG CTG TAT CAA ATC
445 ATT ACG GAT ACC GAA GGT ACT CCG GAT GAA GCG GAC TAC AAA GAC CAT
446 GAC GG 3' and 5' TAC CAT GTA CTG TTT CTC CTC ACA ACG TCT AAA AGA GAC
447 ATT ACC GAA TAA CAT ATG AAT ATC CTC CTT AG 3' and electroporated the

448 resulting PCR product into MG1655 expressing λ Red recombinase from plasmid
449 pKD46 (101), generating strain MJG2179 (*ptsN*-3xFLAG *kan*$^{+}$). We then resolved the
450 kanamycin resistance cassette in MJG2179 with plasmid pCP20 (101) to yield strain
451 MJG2191 (*ptsN*-3xFLAG). We used P1*vir* transduction (24, 100) to move the
452 Δ*phoP790*::*kan*$^{+}$ allele from the Keio collection (43) into MJG2191, generating strain
453 MJG2193 (*ptsN*-3xFLAG Δ*phoP790*::*kan*$^{+}$) We amplified the Δ*rpoN730*::*kan*$^{+}$ allele from
454 strain MJG1763 with primers 5' TAC AAG ACG AAC ACG TTA 3' and 5' TTT GGC AAA
455 TTT GGC TGT 3' and used recombineering (101) to insert this locus into strain
456 MJG2191, generating strain MJG2200 (Δ*rpoN730*::*kan*$^{+}$ *ptsN*-3xFLAG), which we then
457 resolved (101) to generate strain MJG2202 (Δ*rpoN730 ptsN*-3xFLAG).
458
459 **Plasmid construction**
460 Plasmid pRpoN was a gift from Dr. Joseph Wade (NY State Department of
461 Health)(103). We amplified the *glnK* CDS (339 bp) plus 20 bp of upstream sequence
462 from *E. coli* MG1655 genomic DNA with primers 5' TTC GAA TTC ATT CTG ACC GGA
463 GGG GAT CTA T 3' and 5' CTT AAG CTT TTA CAG CGC CGC TTC GTC 3' and
464 cloned it into the *Eco*RI and *Hin*dIII sites of plasmid pBAD18 (58) to generate plasmid
465 pGLNK1. We amplified the *glnB* CDS (339 bp) plus 11 bp of upstream sequence and
466 the *glmS* CDS (1830 bp) plus 25 bp of upstream sequence from *E. coli* MG1655
467 genomic DNA with primers 5' TTT GGG CTA GCG AAT TCC AAG GAA TAG CAT GAA
468 AAA GAT TGA 3' and 5' CAA AAC AGC CAA GCT TTT AAA TTG CCG CGT CGT C 3'
469 or 5' TTT GGG CTA GCG AAT TCA CGA TAT AAA TCG GAA TCA AAA ACT ATG 3'
470 and 5' CAA AAC AGC CAA GCT TTT ACT CAA CCG TAA CCG ATT TTG C 3' and

471 then inserted each gene between the *Eco*RI and *Hin*dIII sites of plasmid pBAD18
472 (amplified with primers 5’ AAG CTT GGC TGT TTT GGC 3’ and 5’ GAA TTC GCT AGC
473 CCA AAA AAA C 3’) by *in vivo* assembly cloning (104) to generate plasmids pGLNB1
474 and pGLMS1, respectively. Plasmid pPPK33, encoding PPK with a C-terminal
475 GAAEPEA peptide tag for affinity purification (105) between the *Nde*I and *Hin*dIII sites
476 of plasmid pET-21b(+)(Novagen), was synthesized by GenScript.
477
478 We amplified the *gfpmut3* CDS (717 bp) (106) with primers 5' TTG AAG GCT CTC AAG
479 GAT GAG TAA AGG AGA AGA ACT TTT CAC TGG 3' and 5' CAG GGC AGG GTC
480 GTT TTA TTT GTA TAG TTC ATC CAT GCC ATG TG 3', the *aadA*$^{+}$ gene and origin of
481 replication of pCDFDuet-1 (Novagen) with primers 5' AAC GAC CCT GCC CTG AAC C
482 3' and 5' CCT TGA GAG CCT TCA ACC CAG T 3', and joined the resulting products by
483 *in vivo* assembly (104), yielding plasmid pGFP3. We amplified the *mgtS* promoter (200
484 bp) from MG1655 genomic DNA with primers 5' GGT TGA AGG CTC TCA AGG TGA
485 TCA TTG CTG CGT GGG TGC TGA 3' and 5' AAG TTC TTC TCC TTT ACT CAT TAT
486 TTG CCT CCG TTT ATG GTG TGG TGT G 3', pGFP3 with primers 5' ATG AGT AAA
487 GGA GAA GAA CTT TTC ACT GGA G 3' and 5' CCT TGA GAG CCT TCA ACC CAG
488 TC 3', and joined the resulting products by *in vivo* assembly (104), yielding plasmid
489 pGFP4.
490
491 We amplified the *ptsN* CDS (492 bp) plus 20 bp of upstream sequence from *E. coli*
492 MG1655 genomic DNA with primers 5' CTC TCT ACT GTT TCT CCA TAC CCG TTT
493 TTT TGG GCT AGC GGC AGG TTC TTA GGT GAA ATT ATG ACA AAT AAT GAT

494 ACA 3' and 5' TAT CAG GCT GAA AAT CTT CTC TCA TCC GCC AAA ACA GCC ACT
495 ACG CTT CAT CCG GAG TAC CT 3' and inserted it between the *Eco*RI and *Hin*dIII
496 sites of plasmid pBAD18 by *in vivo* assembly cloning (104) to generate plasmid
497 pPTSN1. We used single primer site-directed mutagenesis (107) to mutate pPTSN1
498 with primers 5' CAA TGG TAT TGC CAT TCC GGA AGG CAA ACT GGA AGA AGA
499 TAC 3' or 5' GGT ATT GCC ATT CCG GCG GGC AAA CTG GAA GAA G 3'. This
500 yielded pPTSN2, containing a *ptsN*$^{C217G,\ T219A}$ allele (encoding PtsN$^{H73E}$), and pPTSN3,
501 containing a *ptsN*$^{C217G,\ A218C,\ T219G}$ allele (encoding PtsN$^{H73A}$).
502
503 We amplified the dimerizing leucine zipper domain of GCN4 (105 bp) from
504 *Saccharomyces cerevisiae* genomic DNA with primers 5' TCC GGA TCC CTT GCA
505 AAG AAT GAA ACA ACT TGA AG 3' and 5' ACC GGT ACC CGG CGT TCG CCA ACT
506 AAT TTC T 3' and cloned it into the *Bam*HI and *Kpn*I sites of plasmid pKT25 (73) to
507 yield plasmid pGCN4zip1 and into the *Bam*HI and *Kpn*I sites of plasmid pUT18 (73) to
508 yield plasmid pGCN4zip3. We amplified the *ppk* CDS with no stop codon (2084 bp) from
509 *E. coli* MG1655 genomic DNA with primers 5' CAG CTG CAG GGA TGG GTC AGG
510 AAA AGC TAT ACA TCG 3' and 5' TCC GGA TCC TCT TCA GGT TGT TCG AGT GAT
511 TTG 3' and cloned it into the *Pst*I and *Bam*HI sites of plasmid pKNT25 (73) to yield
512 plasmid pPPK12 or into the *Pst*I and *Bam*HI sites of plasmid pKT25 (73) to yield
513 plasmid pPPK13. We amplified the *ptsN* CDS (493 bp) from plasmid pPTSN1 with
514 primers 5' CAC TGC AGG ATG ACA AAT AAT GAT ACA ACT CTA CAG CTT A 3' and
515 5' TGA ATT CGA CTA CGC TTC ATC CGG AGT AC 3', amplified pUT18C (73) with
516 primers 5' GAA GCG TAG TCG AAT TCA TCG ATA TAA CTA AGT AAT ATG GTG 3'

517 and 5' TAT TTG TCA TCC TGC AGT GGC GTT CCA C 3', and joined the resulting
518 products by *in vivo* assembly (104), yielding plasmid pPTSN5.
519
520 **_In vivo_ polyphosphate assay**
521 We extracted and quantified polyP from bacterial cultures as previously described (108).
522 To induce polyP synthesis by nutrient limitation (16, 22), we grew *E. coli* strains in 10 ml
523 rich medium (LB, LBQ, or LBGlcN) at 37°C with shaking (200 rpm) to $A_{600}$=0.2-0.4, then
524 harvested 1 ml samples by centrifugation, resuspended them in 250 µl of 4 M guanidine
525 isothiocyanate, 50 mM Tris-HCl (pH 7), lysed by incubation for 10 min at 95°C, then
526 immediately froze at -80°C. We also harvested 5 ml of each LB culture by centrifugation
527 (5 min at 4,696 g at room temperature), rinsed once with 5 ml phosphate-buffered saline
528 (PBS), then re-centrifuged and resuspended in 5 ml MOPS minimal medium
529 (Teknova)(109) containing 0.1 mM $K_2HPO_4$, and 0.1 mM uracil and 4 g $l^{-1}$ glucose (24).
530 Where indicated, we replaced the glucose with 4 g $l^{-1}$ arabinose, 4 g $l^{-1}$ glucosamine, or
531 8 g $l^{-1}$ glycerol. We incubated these cultures for 2 hours at 37°C with shaking, then
532 collected additional samples as described above. For experiments involving arabinose-
533 inducible plasmids, we added arabinose (2 g $l^{-1}$) to both the rich and minimal media. We
534 determined the protein concentrations of thawed samples by Bradford assay (Bio-Rad)
535 of 5 µl aliquots, then mixed with 250 µl of 95% ethanol, applied to an EconoSpin silica
536 spin column (Epoch Life Science), rinsed with 750 µl 5 mM Tris-HCl, pH 7.5, 50 mM
537 NaCl, 5 mM EDTA, 50% ethanol, then eluted with 150 µl 50 mM Tris-HCl, pH 8. We
538 brought the eluate to 20 mM Tris-HCl, pH 7.5, 5 mM $MgCl_2$, 50 mM ammonium acetate
539 with 1 µg of *Saccharomyces cereviseae* exopolyphosphatase PPX1 (110) in a final

volume of 200 µl, incubated for 15 min at 37°C, then measured the resulting polyP-derived orthophosphate using a colorimetric assay (111) and normalized to total protein content. For all figures, we report polyP concentrations in terms of individual phosphate monomers.

**Quantitative RT-PCR**

At the indicated time points after nutrient limitation, we harvested 1 ml of cells by centrifugation and resuspended in RNA*later* (ThermoFisher) for storage at -20°C. We extracted RNA using the RiboPure™ RNA Purification Kit for bacteria (Ambion) following the manufacturer's instructions, including DNAse treatment to remove contaminating genomic DNA, then used the SuperScript™ IV VILO™ kit (ThermoFisher) to reverse transcribe cDNA from mRNA, following the manufacturer's instructions and including a no-RT control for each reaction. We calculated changes in gene expression using the $2^{-\Delta\Delta Ct}$ method (112), using *yqfB*, whose expression does not change under these polyP induction conditions (22), as an internal expression control.

**PPK overexpression and purification**

C-tagged PPK was overexpressed and purified by a modification of a previously published protocol (17). 50-ml overnight cultures of BL21(DE3) containing pPPK33 were subcultured into 1 l of Protein Expression Media (PEM; 12 g $l^{-1}$ tryptone, 24 g $l^{-1}$ yeast extract, 4% v/v glycerol, 2.314 g $l^{-1}$ $KH_2PO_4$, 12.54 g $l^{-1}$ $K_2HPO_4$) supplemented with 10 mM $MgCl_2$ and 100 µg $ml^{-1}$ ampicillin. The culture was grown at 37°C with shaking until the $A_{600}$ = 0.8, then shifted to 20°C and cooled for 1 hour. Following the cool-down

563 period, PPK expression was induced by the addition of 150 µM isopropyl β-D-1-
564 thiogalactopyranoside (IPTG). Overexpression was allowed to proceed overnight at
565 20°C with shaking. The overexpression culture was pelleted at 6000 g, resuspended in
566 100 ml of Buffer A (50 mM Tris-HCl pH 7.5, 10% w/v sucrose) with 300 µg $ml^{-1}$
567 lysozyme, and incubated on ice for 45 min. The digest was pelleted at 16,000 x g for 10
568 minutes, then the pellet was resuspended in 50 ml of Buffer B (Buffer A + 5 mM $MgCl_2$ +
569 30 U $ml^{-1}$ Pierce Universal Nuclease + 1 Pierce Protease Inhibitor cocktail tablet) and
570 lysed by sonication (5 s on, 5 s off for 5 min at 50% amplitude). The sonicated lysate
571 was pelleted at 20,000 g for 1 hour at 4°C, and the pellet was resuspended in 25 ml of
572 C-tag Binding Buffer (20 mM Tris-HCl pH 7.4) plus solid KCl to 1 M final concentration.
573 1 M $Na_2CO_3$ was added at a 1:10 dilution to the resuspension, and the salt extraction
574 was incubated at 4°C for 30 min with stirring. Following incubation, the solution was
575 sonicated in 5 s pulses for 2 min, then pelleted at 20,000 g for 1 hour at 4°C. The
576 supernatant was diluted 1:1 with cold $H_2O$ and loaded onto a C-tag Affinity Column
577 (ThermoFisher) equilibrated with C-tag Binding Buffer. The column was washed with 10
578 column volumes of C-tag Binding Buffer and PPK was eluted with a gradient of 0-100%
579 C-tag Elution Buffer (20 mM Tris-HCl pH 7.4, 2 M $MgCl_2$) with an ÄKTA™ Start FPLC
580 (Cytiva Life Sciences). Fractions containing pure PPK were pooled and dialyzed against
581 PPK Storage Buffer (20 mM HEPES-KOH pH 8.0, 150 mM NaCl, 15% glycerol, 1 mM
582 EDTA) at 4°C and stored at -80°C.
583
584 ***In vitro* assay of PPK activity**

We determined the specific activity for polyP synthesis by PPK as previously described (23). Reactions (125 µl total volume) contained 5 nM PPK, 50 mM HEPES-KOH (pH 7.5), 50 mM ammonium sulfate, 5 mM $MgCl_2$, 20 mM creatine phosphate, and 60 µg $ml^{-1}$ creatine kinase. Where indicated, reactions also contained 100 mM *L*-glutamate (pH 7.5), 10 mM *L*-glutamine (pH 7.5), 1 mM fructose-6-phosphate, 1 mM glucosamine-6-phosphate, or 5 or 10 mM α-ketoglutarate (pH 7.5), concentrations chosen to represent the high end of the physiological range for each compound in *E. coli* (51). We prewarmed reactions to 37°C, then started them by addition of MgATP to a final concentration of 6 mM. We removed aliquots (20 µl) at 1, 2, 3, and 4 minutes and diluted them into 80 µl of a stop solution containing 62.5 mM EDTA and 50 µM DAPI (4',6-diamidino-2-phenylindole) in black 96-well plates, then measured steady-state polyP-DAPI fluorescence of these samples (ex. 415 nm, em. 600 nm) (15) in an Infinite M1000 Pro microplate reader (Tecan Group, Ltd.). We determined the polyP content of each sample (calculated in terms of individual phosphate monomers) by comparison to a standard curve of commercially available polyP (Acros Organics) (0 - 150 µM) prepared in the buffer described above containing 6 mM MgATP and calculated rates of polyP synthesis by linear regression (Prism 9, GraphPad Software, Inc.).

**Bacterial two-hybrid protein interaction assay**

We assessed protein interactions *in vivo* using the BACTH procedure (73). Briefly, we grew derivatives of *E. coli cya* strain BTH101 containing plasmids expressing fusions of proteins of interest to the T18 or T25 complementary fragments of *Bordetella pertussis* adenylate cyclase overnight in LB and then evaluated β-galactosidase activity of these

608 strains either by spotting overnight cultures on LB plates containing ampicillin,
609 kanamycin, 0.5 mM IPTG, and 40 µg $ml^{-1}$ 5-bromo-4-chloro-3-indolyl-β-D-
610 galactopyranoside (X-Gal) and incubating for 2 days at 30°C or, for quantitative
611 measurements, using a single-step assay (113): after 24 h of growth at 37°C in LB broth
612 containing ampicillin, kanamycin, and 0.5 mM IPTG we harvested 80 µL of cells by
613 centrifugation, resuspended them in 200 µL of 60 mM $Na_2HPO_4$, 40 mM $NaH_2PO_4$, 10
614 mM KCl, 1 mM $MgSO_4$, 36 mM β-mercaptoethanol, 1.1 mg $ml^{-1}$ *ortho*-nitrophenyl-β-
615 galactoside (ONPG), 1.25 mg $ml^{-1}$ lysozyme and 6.7% PopCulture reagent (Novagen) in
616 a 96-well plate, and then measured $A_{600}$ and $A_{420}$ over time at 24°C in a Tecan M1000
617 Infinite plate reader. We calculated Miller Units according to the formula (1000 x ($A_{420}$ /
618 min)) / (initial $A_{600}$ x culture volume (ml)).
619
620 **Quantitative Western blotting**
621 *E. coli* strains with chromosomal *ptsN*-3xFLAG fusions were grown and stressed by
622 nutrient limitation as described above. At the indicated time points, 1-ml aliquots were
623 harvested by centrifugation and resuspended in 100 µl of 50 mM Tris-HCl (pH 8), 150
624 mM NaCl, 1% Triton X-100 containing 1X HALT protease inhibitor cocktail
625 (ThermoFisher), then incubated at 95°C for 10 min to lyse the cells. Lysates were stored
626 at -80°C until use. Aliquots of each sample were thawed on ice, mixed 1:1 with fresh
627 lysis buffer, then mixed 4:1 with reducing loading dye (250 mM Tris-HCl pH 6.8, 10%
628 SDS, 0.008% bromophenol blue, 40% glycerol, 2.8 M β-mercaptoethanol). Western
629 blots were prepared and analyzed as described previously (114, 115) with few
630 exceptions. Briefly, lysate samples were loaded on an AnykDa Stain-Free SDS-PAGE

gel (BioRad Cat #4568126) and run until the dye front neared the bottom of the gel. Gels were then transferred to a PVDF membrane (BioRad Cat # 1620174) using a TurboBlot semi-dry transfer system, then blocked in StartingBlock T20 TBS blocking buffer (Thermo Cat #37543) overnight. Blots were blocked for 30 min at room temperature, then incubated in a 1:25,000 dilution of rabbit anti-RecA antibody (Abcam Cat #ab63797) in the blocking buffer for one hour at room temperature. Blots were washed in three times in TBST, then incubated 1 hour at room temperature in blocking buffer containing a 1:10,000 dilution of goat anti-Rabbit IgG H+L HRP-conjugated (Abcam Cat #ab63797). Blots were washed again in 3X TBS-T then incubated in blocking buffer containing a 1:5000 dilution of rabbit Anti-DDDDK HRP conjugated antibody (Abcam Cat #ab2493). Blots were washed three times with TBST and once with TBS, then developed using the BioRad Clarity ECL Substrate kit (Cat # 1705061) and imaged on a BioRad Gel Doc. Images were analyzed in ImageJ (116) by taking same-area measurements of each RecA band or PtsN band, blank correcting the mean gray values (signal) using same-area measurements matched to the respective band, and normalizing the PtsN signal to RecA signal.

**Statistical analyses**

We used GraphPad Prism version 9.2 (GraphPad Software) to perform statistical analyses, including two-way repeated measures ANOVA with Holm-Sidak's multiple comparison tests. Repeated measures ANOVA cannot handle missing values, so we analyzed data sets with samples having different *n* numbers (*e.g.* Fig. 1C) with an

equivalent mixed model which uses a compound symmetry covariance matrix and is fit using Restricted Maximum Likelihood (REML) (without Geisser-Greenhouse correction).

## Data availability

All strains and plasmids generated in the course of this work are available from the authors upon request.

## ACKNOWLEDGEMENTS

This project was supported by NIH grant R35GM124590.

## REFERENCES

1. Denoncourt A, Downey M. 2021. Model systems for studying polyphosphate biology: a focus on microorganisms. Curr Genet doi:10.1007/s00294-020-01148-x.
2. Desfougeres Y, Saiardi A, Azevedo C. 2020. Inorganic polyphosphate in mammals: where's Wally? Biochem Soc Trans 48:95-101.
3. Albi T, Serrano A. 2016. Inorganic polyphosphate in the microbial world. Emerging roles for a multifaceted biopolymer. World J Microbiol Biotechnol 32:27.
4. Gautam LK, Sharma P, Capalash N. 2019. Bacterial Polyphosphate Kinases Revisited: Role in Pathogenesis and Therapeutic Potential. Curr Drug Targets 20:292-301.

5. Rao NN, Gomez-Garcia MR, Kornberg A. 2009. Inorganic polyphosphate: essential for growth and survival. Annu Rev Biochem 78:605-47.

6. Gray MJ, Jakob U. 2015. Oxidative stress protection by polyphosphate--new roles for an old player. Curr Opin Microbiol 24:1-6.

7. Bowlin MQ, Gray MJ. 2021. Inorganic Polyphosphate in Host and Microbe Biology. Trends Microbiol doi:10.1016/j.tim.2021.02.002:S0966-842X(21)00036-6.

8. Suess PM, Chinea LE, Pilling D, Gomer RH. 2019. Extracellular Polyphosphate Promotes Macrophage and Fibrocyte Differentiation, Inhibits Leukocyte Proliferation, and Acts as a Chemotactic Agent for Neutrophils. J Immunol 203:493-499.

9. Roewe J, Stavrides G, Strueve M, Sharma A, Marini F, Mann A, Smith SA, Kaya Z, Strobl B, Mueller M, Reinhardt C, Morrissey JH, Bosmann M. 2020. Bacterial polyphosphates interfere with the innate host defense to infection. Nat Commun 11:4035.

10. Rijal R, Cadena LA, Smith MR, Carr JF, Gomer RH. 2020. Polyphosphate is an extracellular signal that can facilitate bacterial survival in eukaryotic cells. Proceedings of the National Academy of Sciences doi:10.1073/pnas.2012009117:202012009.

11. McDonald B, Davis RP, Kim SJ, Tse M, Esmon CT, Kolaczkowska E, Jenne CN. 2017. Platelets and neutrophil extracellular traps collaborate to promote intravascular coagulation during sepsis in mice. Blood 129:1357-1367.

12. Peng L, Zeng L, Jin H, Yang L, Xiao Y, Lan Z, Yu Z, Ouyang S, Zhang L, Sun N. 2020. Discovery and antibacterial study of potential PPK1 inhibitors against uropathogenic E. coli. J Enzyme Inhib Med Chem 35:1224-1232.

13. Neville N, Roberge N, Ji X, Stephen P, Lu JL, Jia Z. 2021. A Dual-Specificity Inhibitor Targets Polyphosphate Kinase 1 and 2 Enzymes To Attenuate Virulence of Pseudomonas aeruginosa. mBio 12:e0059221.

14. Bravo-Toncio C, Alvarez JA, Campos F, Ortiz-Severin J, Varas M, Cabrera R, Lagos CF, Chavez FP. 2016. Dictyostelium discoideum as a surrogate host-microbe model for antivirulence screening in Pseudomonas aeruginosa PAO1. Int J Antimicrob Agents 47:403-9.

15. Dahl JU, Gray MJ, Bazopoulou D, Beaufay F, Lempart J, Koenigsknecht MJ, Wang Y, Baker JR, Hasler WL, Young VB, Sun D, Jakob U. 2017. The anti-inflammatory drug mesalamine targets bacterial polyphosphate accumulation. Nat Microbiol 2:16267.

16. Ault-Riche D, Fraley CD, Tzeng CM, Kornberg A. 1998. Novel assay reveals multiple pathways regulating stress-induced accumulations of inorganic polyphosphate in Escherichia coli. J Bacteriol 180:1841-7.

17. Gray MJ, Wholey WY, Wagner NO, Cremers CM, Mueller-Schickert A, Hock NT, Krieger AG, Smith EM, Bender RA, Bardwell JC, Jakob U. 2014. Polyphosphate is a primordial chaperone. Mol Cell 53:689-99.

18. Yoo NG, Dogra S, Meinen BA, Tse E, Haefliger J, Southworth DR, Gray MJ, Dahl JU, Jakob U. 2018. Polyphosphate Stabilizes Protein Unfolding Intermediates as Soluble Amyloid-like Oligomers. J Mol Biol 430:4195-4208.

19. Morohoshi T, Maruo T, Shirai Y, Kato J, Ikeda T, Takiguchi N, Ohtake H, Kuroda A. 2002. Accumulation of inorganic polyphosphate in phoU mutants of Escherichia coli and Synechocystis sp. strain PCC6803. Appl Environ Microbiol 68:4107-10.

20. Kuroda A, Murphy H, Cashel M, Kornberg A. 1997. Guanosine tetra- and pentaphosphate promote accumulation of inorganic polyphosphate in Escherichia coli. J Biol Chem 272:21240-3.

21. Akiyama M, Crooke E, Kornberg A. 1993. An exopolyphosphatase of Escherichia coli. The enzyme and its ppx gene in a polyphosphate operon. J Biol Chem 268:633-9.

22. Gray MJ. 2020. Interactions between DksA and Stress-Responsive Alternative Sigma Factors Control Inorganic Polyphosphate Accumulation in Escherichia coli. J Bacteriol 202:e00133-20.

23. Rudat AK, Pokhrel A, Green TJ, Gray MJ. 2018. Mutations in Escherichia coli Polyphosphate Kinase That Lead to Dramatically Increased In Vivo Polyphosphate Levels. J Bacteriol 200:e00697-17.

24. Gray MJ. 2019. Inorganic Polyphosphate Accumulation in Escherichia coli Is Regulated by DksA but Not by (p)ppGpp. J Bacteriol 201:e00664-18.

25. Danson AE, Jovanovic M, Buck M, Zhang X. 2019. Mechanisms of sigma(54)-Dependent Transcription Initiation and Regulation. J Mol Biol 431:3960-3974.

26. Riordan JT, Mitra A. 2017. Regulation of Escherichia coli Pathogenesis by Alternative Sigma Factor N. EcoSal Plus 7.

742 27. Keseler IM, Mackie A, Santos-Zavaleta A, Billington R, Bonavides-Martinez C,
743 Caspi R, Fulcher C, Gama-Castro S, Kothari A, Krummenacker M, Latendresse
744 M, Muniz-Rascado L, Ong Q, Paley S, Peralta-Gil M, Subhraveti P, Velazquez-
745 Ramirez DA, Weaver D, Collado-Vides J, Paulsen I, Karp PD. 2017. The EcoCyc
746 database: reflecting new knowledge about Escherichia coli K-12. Nucleic Acids
747 Res 45:D543-D550.
748 28. van Heeswijk WC, Westerhoff HV, Boogerd FC. 2013. Nitrogen assimilation in
749 Escherichia coli: putting molecular data into a systems perspective. Microbiol Mol
750 Biol Rev 77:628-95.
751 29. Khan MA, Durica-Mitic S, Gopel Y, Heermann R, Gorke B. 2020. Small RNA-
752 binding protein RapZ mediates cell envelope precursor sensing and signaling in
753 Escherichia coli. EMBO J 39:e103848.
754 30. Gopel Y, Gorke B. 2018. Interaction of lipoprotein QseG with sensor kinase
755 QseE in the periplasm controls the phosphorylation state of the two-component
756 system QseE/QseF in Escherichia coli. PLoS Genet 14:e1007547.
757 31. Reichenbach B, Gopel Y, Gorke B. 2009. Dual control by perfectly overlapping
758 sigma 54- and sigma 70- promoters adjusts small RNA GlmY expression to
759 different environmental signals. Mol Microbiol 74:1054-70.
760 32. Klein G, Stupak A, Biernacka D, Wojtkiewicz P, Lindner B, Raina S. 2016.
761 Multiple Transcriptional Factors Regulate Transcription of the rpoE Gene in
762 Escherichia coli under Different Growth Conditions and When the
763 Lipopolysaccharide Biosynthesis Is Defective. J Biol Chem 291:22999-23019.

764 33. Groisman EA, Duprey A, Choi J. 2021. How the PhoP/PhoQ System Controls
765 Virulence and Mg(2+) Homeostasis: Lessons in Signal Transduction,
766 Pathogenesis, Physiology, and Evolution. Microbiol Mol Biol Rev 85:e0017620.
767 34. Pfluger-Grau K, Gorke B. 2010. Regulatory roles of the bacterial nitrogen-related
768 phosphotransferase system. Trends Microbiol 18:205-14.
769 35. Racki LR, Tocheva EI, Dieterle MG, Sullivan MC, Jensen GJ, Newman DK.
770 2017. Polyphosphate granule biogenesis is temporally and functionally tied to cell
771 cycle exit during starvation in Pseudomonas aeruginosa. Proc Natl Acad Sci U S
772 A 114:E2440-E2449.
773 36. Ikeda TP, Shauger AE, Kustu S. 1996. Salmonella typhimurium apparently
774 perceives external nitrogen limitation as internal glutamine limitation. J Mol Biol
775 259:589-607.
776 37. Huergo LF, Dixon R. 2015. The Emergence of 2-Oxoglutarate as a Master
777 Regulator Metabolite. Microbiol Mol Biol Rev 79:419-35.
778 38. Forchhammer K, Luddecke J. 2016. Sensory properties of the PII signalling
779 protein family. FEBS J 283:425-37.
780 39. Blauwkamp TA, Ninfa AJ. 2002. Physiological role of the GlnK signal
781 transduction protein of Escherichia coli: survival of nitrogen starvation. Mol
782 Microbiol 46:203-14.
783 40. Maeda K, Westerhoff HV, Kurata H, Boogerd FC. 2019. Ranking network
784 mechanisms by how they fit diverse experiments and deciding on E. coli's
785 ammonium transport and assimilation network. NPJ Syst Biol Appl 5:14.

786 41. Gosztolai A, Schumacher J, Behrends V, Bundy JG, Heydenreich F, Bennett MH,
787 Buck M, Barahona M. 2017. GlnK Facilitates the Dynamic Regulation of Bacterial
788 Nitrogen Assimilation. Biophys J 112:2219-2230.
789 42. Atkinson MR, Blauwkamp TA, Ninfa AJ. 2002. Context-dependent functions of
790 the PII and GlnK signal transduction proteins in Escherichia coli. J Bacteriol
791 184:5364-75.
792 43. Baba T, Ara T, Hasegawa M, Takai Y, Okumura Y, Baba M, Datsenko KA,
793 Tomita M, Wanner BL, Mori H. 2006. Construction of Escherichia coli K-12 in-
794 frame, single-gene knockout mutants: the Keio collection. Mol Syst Biol 2:2006
795 0008.
796 44. He B, Choi KY, Zalkin H. 1993. Regulation of Escherichia coli glnB, prsA, and
797 speA by the purine repressor. J Bacteriol 175:3598-606.
798 45. Santos-Zavaleta A, Salgado H, Gama-Castro S, Sanchez-Perez M, Gomez-
799 Romero L, Ledezma-Tejeida D, Garcia-Sotelo JS, Alquicira-Hernandez K, Muniz-
800 Rascado LJ, Pena-Loredo P, Ishida-Gutierrez C, Velazquez-Ramirez DA, Del
801 Moral-Chavez V, Bonavides-Martinez C, Mendez-Cruz CF, Galagan J, Collado-
802 Vides J. 2019. RegulonDB v 10.5: tackling challenges to unify classic and high
803 throughput knowledge of gene regulation in E. coli K-12. Nucleic Acids Res
804 47:D212-D220.
805 46. Blauwkamp TA, Ninfa AJ. 2003. Antagonism of PII signalling by the AmtB protein
806 of Escherichia coli. Mol Microbiol 48:1017-28.
807 47. Rodionova IA, Goodacre N, Babu M, Emili A, Uetz P, Saier MH, Jr. 2018. The
808 Nitrogen Regulatory PII Protein (GlnB) and N-Acetylglucosamine 6-Phosphate

809 Epimerase (NanE) Allosterically Activate Glucosamine 6-Phosphate Deaminase
810 (NagB) in Escherichia coli. J Bacteriol 200.
811 48. Schubert C, Zedler S, Strecker A, Unden G. 2021. L-Aspartate as a high-quality
812 nitrogen source in Escherichia coli: Regulation of L-aspartase by the nitrogen
813 regulatory system and interaction of L-aspartase with GlnB. Mol Microbiol
814 115:526-538.
815 49. Atkinson MR, Ninfa AJ. 1998. Role of the GlnK signal transduction protein in the
816 regulation of nitrogen assimilation in Escherichia coli. Mol Microbiol 29:431-47.
817 50. Sezonov G, Joseleau-Petit D, D'Ari R. 2007. Escherichia coli physiology in Luria-
818 Bertani broth. J Bacteriol 189:8746-9.
819 51. Bennett BD, Kimball EH, Gao M, Osterhout R, Van Dien SJ, Rabinowitz JD.
820 2009. Absolute metabolite concentrations and implied enzyme active site
821 occupancy in Escherichia coli. Nat Chem Biol 5:593-9.
822 52. Yakhnin H, Aichele R, Ades SE, Romeo T, Babitzke P. 2017. Circuitry Linking
823 the Global Csr- and sigma(E)-Dependent Cell Envelope Stress Response
824 Systems. J Bacteriol 199.
825 53. Hews CL, Cho T, Rowley G, Raivio TL. 2019. Maintaining Integrity Under Stress:
826 Envelope Stress Response Regulation of Pathogenesis in Gram-Negative
827 Bacteria. Front Cell Infect Microbiol 9:313.
828 54. Durica-Mitic S, Gopel Y, Amman F, Gorke B. 2020. Adaptor protein RapZ
829 activates endoribonuclease RNase E by protein-protein interaction to cleave a
830 small regulatory RNA. RNA 26:1198-1215.

831 55. Teplyakov A, Leriche C, Obmolova G, Badet B, Badet-Denisot MA. 2002. From
832 Lobry de Bruyn to enzyme-catalyzed ammonia channelling: molecular studies of
833 D-glucosamine-6P synthase. Nat Prod Rep 19:60-9.
834 56. Mouilleron S, Badet-Denisot MA, Badet B, Golinelli-Pimpaneau B. 2011.
835 Dynamics of glucosamine-6-phosphate synthase catalysis. Arch Biochem
836 Biophys 505:1-12.
837 57. Wang H, Yin X, Wu Orr M, Dambach M, Curtis R, Storz G. 2017. Increasing
838 intracellular magnesium levels with the 31-amino acid MgtS protein. Proc Natl
839 Acad Sci U S A 114:5689-5694.
840 58. Guzman LM, Belin D, Carson MJ, Beckwith J. 1995. Tight regulation, modulation,
841 and high-level expression by vectors containing the arabinose PBAD promoter. J
842 Bacteriol 177:4121-30.
843 59. Alvarez-Anorve LI, Bustos-Jaimes I, Calcagno ML, Plumbridge J. 2009. Allosteric
844 regulation of glucosamine-6-phosphate deaminase (NagB) and growth of
845 Escherichia coli on glucosamine. J Bacteriol 191:6401-7.
846 60. Kalamorz F, Reichenbach B, Marz W, Rak B, Gorke B. 2007. Feedback control
847 of glucosamine-6-phosphate synthase GlmS expression depends on the small
848 RNA GlmZ and involves the novel protein YhbJ in Escherichia coli. Mol Microbiol
849 65:1518-33.
850 61. Plumbridge JA, Cochet O, Souza JM, Altamirano MM, Calcagno ML, Badet B.
851 1993. Coordinated regulation of amino sugar-synthesizing and -degrading
852 enzymes in Escherichia coli K-12. J Bacteriol 175:4951-6.

853 62. Choi J, Kim H, Chang Y, Yoo W, Kim D, Ryu S. 2019. Programmed Delay of a
854 Virulence Circuit Promotes Salmonella Pathogenicity. mBio 10.
855 63. Yoo W, Choi J, Park B, Byndloss MX, Ryu S. 2021. A Nitrogen Metabolic
856 Enzyme Provides Salmonella Fitness Advantage by Promoting Utilization of
857 Microbiota-Derived Carbon Source. ACS Infect Dis
858 doi:10.1021/acsinfecdis.0c00836.
859 64. Yoo W, Yoon H, Seok YJ, Lee CR, Lee HH, Ryu S. 2016. Fine-tuning of amino
860 sugar homeostasis by EIIA(Ntr) in Salmonella Typhimurium. Sci Rep 6:33055.
861 65. Kim HJ, Lee CR, Kim M, Peterkofsky A, Seok YJ. 2011. Dephosphorylated NPr
862 of the nitrogen PTS regulates lipid A biosynthesis by direct interaction with LpxD.
863 Biochem Biophys Res Commun 409:556-61.
864 66. Lee J, Park YH, Kim YR, Seok YJ, Lee CR. 2015. Dephosphorylated NPr is
865 involved in an envelope stress response of Escherichia coli. Microbiology
866 (Reading) 161:1113-1123.
867 67. Choi J, Ryu S. 2019. Regulation of Iron Uptake by Fine-Tuning the Iron
868 Responsiveness of the Iron Sensor Fur. Appl Environ Microbiol 85.
869 68. Deutscher J, Ake FM, Derkaoui M, Zebre AC, Cao TN, Bouraoui H, Kentache T,
870 Mokhtari A, Milohanic E, Joyet P. 2014. The bacterial
871 phosphoenolpyruvate:carbohydrate phosphotransferase system: regulation by
872 protein phosphorylation and phosphorylation-dependent protein-protein
873 interactions. Microbiol Mol Biol Rev 78:231-56.

874 69. Lee CR, Park YH, Kim M, Kim YR, Park S, Peterkofsky A, Seok YJ. 2013.
875 Reciprocal regulation of the autophosphorylation of enzyme INtr by glutamine
876 and alpha-ketoglutarate in Escherichia coli. Mol Microbiol 88:473-85.
877 70. Rabus R, Reizer J, Paulsen I, Saier MH, Jr. 1999. Enzyme I(Ntr) from
878 Escherichia coli. A novel enzyme of the phosphoenolpyruvate-dependent
879 phosphotransferase system exhibiting strict specificity for its phosphoryl
880 acceptor, NPr. J Biol Chem 274:26185-91.
881 71. Karstens K, Zschiedrich CP, Bowien B, Stulke J, Gorke B. 2014.
882 Phosphotransferase protein EIIANtr interacts with SpoT, a key enzyme of the
883 stringent response, in Ralstonia eutropha H16. Microbiology (Reading) 160:711-
884 722.
885 72. Mork-Morkenstein M, Heermann R, Gopel Y, Jung K, Gorke B. 2017. Non-
886 canonical activation of histidine kinase KdpD by phosphotransferase protein PtsN
887 through interaction with the transmitter domain. Mol Microbiol 106:54-73.
888 73. Karimova G, Pidoux J, Ullmann A, Ladant D. 1998. A bacterial two-hybrid system
889 based on a reconstituted signal transduction pathway. Proc Natl Acad Sci U S A
890 95:5752-6.
891 74. Rhodius VA, Suh WC, Nonaka G, West J, Gross CA. 2006. Conserved and
892 variable functions of the sigmaE stress response in related genomes. PLoS Biol
893 4:e2.
894 75. Hayden JD, Ades SE. 2008. The extracytoplasmic stress factor, sigmaE, is
895 required to maintain cell envelope integrity in Escherichia coli. PLoS One
896 3:e1573.

897 76. Costanzo A, Nicoloff H, Barchinger SE, Banta AB, Gourse RL, Ades SE. 2008.
898 ppGpp and DksA likely regulate the activity of the extracytoplasmic stress factor
899 sigmaE in Escherichia coli by both direct and indirect mechanisms. Mol Microbiol
900 67:619-32.
901 77. Loffler M, Simen JD, Muller J, Jager G, Laghrami S, Schaferhoff K, Freund A,
902 RecogNice T, Takors R. 2017. Switching between nitrogen and glucose
903 limitation: Unraveling transcriptional dynamics in Escherichia coli. J Biotechnol
904 258:2-12.
905 78. Wang L, Yan J, Wise MJ, Liu Q, Asenso J, Huang Y, Dai S, Liu Z, Du Y, Tang D.
906 2018. Distribution Patterns of Polyphosphate Metabolism Pathway and Its
907 Relationships With Bacterial Durability and Virulence. Front Microbiol 9:782.
908 79. Achbergerova L, Nahalka J. 2011. Polyphosphate--an ancient energy source and
909 active metabolic regulator. Microb Cell Fact 10:63.
910 80. Gottesman S. 2019. Trouble is coming: Signaling pathways that regulate general
911 stress responses in bacteria. J Biol Chem 294:11685-11700.
912 81. Schellhorn HE. 2020. Function, Evolution, and Composition of the RpoS Regulon
913 in Escherichia coli. Front Microbiol 11:560099.
914 82. Saha S, Lach SR, Konovalova A. 2021. Homeostasis of the Gram-negative cell
915 envelope. Curr Opin Microbiol 61:99-106.
916 83. Luttmann D, Gopel Y, Gorke B. 2012. The phosphotransferase protein EIIA(Ntr)
917 modulates the phosphate starvation response through interaction with histidine
918 kinase PhoR in Escherichia coli. Mol Microbiol 86:96-110.

919 84. Luttmann D, Heermann R, Zimmer B, Hillmann A, Rampp IS, Jung K, Gorke B.
920 2009. Stimulation of the potassium sensor KdpD kinase activity by interaction
921 with the phosphotransferase protein IIA(Ntr) in Escherichia coli. Mol Microbiol
922 72:978-94.
923 85. Lee CR, Cho SH, Kim HJ, Kim M, Peterkofsky A, Seok YJ. 2010. Potassium
924 mediates Escherichia coli enzyme IIA(Ntr) -dependent regulation of sigma factor
925 selectivity. Mol Microbiol 78:1468-83.
926 86. Lee CR, Cho SH, Yoon MJ, Peterkofsky A, Seok YJ. 2007. Escherichia coli
927 enzyme IIANtr regulates the K+ transporter TrkA. Proc Natl Acad Sci U S A
928 104:4124-9.
929 87. Grillo-Puertas M, Rintoul MR, Rapisarda VA. 2016. PhoB activation in non-
930 limiting phosphate condition by the maintenance of high polyphosphate levels in
931 the stationary phase inhibits biofilm formation in Escherichia coli. Microbiology
932 (Reading) 162:1000-1008.
933 88. Hirota R, Motomura K, Nakai S, Handa T, Ikeda T, Kuroda A. 2013. Stable
934 polyphosphate accumulation by a pseudo-revertant of an Escherichia coli phoU
935 mutant. Biotechnol Lett 35:695-701.
936 89. Gravina F, Degaut FL, Gerhardt ECM, Pedrosa FO, Souza EM, Antonio de
937 Souza G, Huergo LF. 2021. The protein-protein interaction network of the
938 Escherichia coli EIIA(Ntr) regulatory protein reveals a role in cell motility and
939 metabolic control. Res Microbiol doi:10.1016/j.resmic.2021.103882:103882.

940 90. Zwir I, Shin D, Kato A, Nishino K, Latifi T, Solomon F, Hare JM, Huang H,
941 Groisman EA. 2005. Dissecting the PhoP regulatory network of Escherichia coli
942 and Salmonella enterica. Proc Natl Acad Sci U S A 102:2862-7.
943 91. Yeom J, Gao X, Groisman EA. 2018. Reduction in adaptor amounts establishes
944 degradation hierarchy among protease substrates. Proc Natl Acad Sci U S A
945 115:E4483-E4492.
946 92. Yeom J, Groisman EA. 2021. Reduced ATP-dependent proteolysis of functional
947 proteins during nutrient limitation speeds the return of microbes to a growth state.
948 Sci Signal 14.
949 93. Ahn K, Kornberg A. 1990. Polyphosphate kinase from Escherichia coli.
950 Purification and demonstration of a phosphoenzyme intermediate. J Biol Chem
951 265:11734-9.
952 94. Guo B, Bi Y. 2002. Cloning PCR products. An overview. Methods Mol Biol
953 192:111-9.
954 95. Sambrook J, Fritsch EF, Maniatis T. 1989. Molecular Cloning: A Laboratory
955 Manual, 2 ed. Cold Spring Harbor Laboratory Press, Cold Spring Harbor, NY.
956 96. Bertani G. 1951. Studies on lysogenesis. I. The mode of phage liberation by
957 lysogenic Escherichia coli. J Bacteriol 62:293-300.
958 97. Daimon Y, Narita S, Akiyama Y. 2015. Activation of Toxin-Antitoxin System
959 Toxins Suppresses Lethality Caused by the Loss of sigmaE in Escherichia coli. J
960 Bacteriol 197:2316-24.
961 98. Chen IA, Chu K, Palaniappan K, Ratner A, Huang J, Huntemann M, Hajek P,
962 Ritter S, Varghese N, Seshadri R, Roux S, Woyke T, Eloe-Fadrosh EA, Ivanova

963 NN, Kyrpides NC. 2021. The IMG/M data management and analysis system
964 v.6.0: new tools and advanced capabilities. Nucleic Acids Res 49:D751-D763.
965 99. Blattner FR, Plunkett G, 3rd, Bloch CA, Perna NT, Burland V, Riley M, Collado-
966 Vides J, Glasner JD, Rode CK, Mayhew GF, Gregor J, Davis NW, Kirkpatrick
967 HA, Goeden MA, Rose DJ, Mau B, Shao Y. 1997. The complete genome
968 sequence of Escherichia coli K-12. Science 277:1453-62.
969 100. Silhavy TJ, Berman ML, Enquist LW. 1984. Experiments with gene fusions. Cold
970 Spring Harbor Laboratory, Cold Spring Harbor, NY.
971 101. Datsenko KA, Wanner BL. 2000. One-step inactivation of chromosomal genes in
972 Escherichia coli K-12 using PCR products. Proc Natl Acad Sci U S A 97:6640-5.
973 102. Uzzau S, Figueroa-Bossi N, Rubino S, Bossi L. 2001. Epitope tagging of
974 chromosomal genes in Salmonella. Proc Natl Acad Sci U S A 98:15264-9.
975 103. Bonocora RP, Smith C, Lapierre P, Wade JT. 2015. Genome-Scale Mapping of
976 Escherichia coli sigma54 Reveals Widespread, Conserved Intragenic Binding.
977 PLoS Genet 11:e1005552.
978 104. Watson JF, Garcia-Nafria J. 2019. In vivo DNA assembly using common
979 laboratory bacteria: A re-emerging tool to simplify molecular cloning. J Biol Chem
980 294:15271-15281.
981 105. De Genst EJ, Guilliams T, Wellens J, O'Day EM, Waudby CA, Meehan S,
982 Dumoulin M, Hsu ST, Cremades N, Verschueren KH, Pardon E, Wyns L,
983 Steyaert J, Christodoulou J, Dobson CM. 2010. Structure and properties of a
984 complex of alpha-synuclein and a single-domain camelid antibody. J Mol Biol
985 402:326-43.

106. Cormack BP, Valdivia RH, Falkow S. 1996. FACS-optimized mutants of the green fluorescent protein (GFP). Gene 173:33-8.

107. Huang Y, Zhang L. 2017. An In Vitro Single-Primer Site-Directed Mutagenesis Method for Use in Biotechnology. Methods Mol Biol 1498:375-383.

108. Pokhrel A, Lingo JC, Wolschendorf F, Gray MJ. 2019. Assaying for Inorganic Polyphosphate in Bacteria. J Vis Exp doi:10.3791/58818:e58818.

109. Neidhardt FC, Bloch PL, Smith DF. 1974. Culture medium for enterobacteria. J Bacteriol 119:736-47.

110. Wurst H, Kornberg A. 1994. A soluble exopolyphosphatase of Saccharomyces cerevisiae. Purification and characterization. J Biol Chem 269:10996-1001.

111. Christ JJ, Blank LM. 2018. Enzymatic quantification and length determination of polyphosphate down to a chain length of two. Anal Biochem 548:82-90.

112. Schmittgen TD, Livak KJ. 2008. Analyzing real-time PCR data by the comparative C(T) method. Nat Protoc 3:1101-8.

113. Schaefer J, Jovanovic G, Kotta-Loizou I, Buck M. 2016. Single-step method for beta-galactosidase assays in Escherichia coli using a 96-well microplate reader. Anal Biochem 503:56-7.

114. Pillai-Kastoori L, Schutz-Geschwender AR, Harford JA. 2020. A systematic approach to quantitative Western blot analysis. Anal Biochem 593:113608.

115. Kurien BT, Scofield RH. 2009. Introduction to protein blotting. Methods Mol Biol 536:9-22.

116. Schneider CA, Rasband WS, Eliceiri KW. 2012. NIH Image to ImageJ: 25 years of image analysis. Nat Methods 9:671-5.

**TABLE 1.** Strains and plasmids used in this study. Unless otherwise indicated, all strains and plasmids were generated in the course of this work. Abbreviations: $Ap^R$, ampicillin resistance; $Cm^R$, chloramphenicol resistance; $Em^D$, erythromycin dependance; $Gm^R$, gentamycin resistance; $Kn^R$, kanamycin resistance; $Sp^R$, spectinomycin resistance; $Sm^R$, streptomycin resistance.

| Strain | Marker(s) | Relevant Genotype | Source |
|---|---|---|---|
| *E. coli* strains: | | | |
| DH5α | | $F^-$, λ$^-$, ϕ80*lacZ*ΔM15 Δ(*lacZYA-argF*)*U169* *recA1 endA1 hsdR17*($r_K^-$, $m_K^+$) *phoA supE44* *thi-1 gyrA96 relA1* | Invitrogen |
| BL21(DE3) | | $F^-$, *ompT gal dcm lon hsdSB*($r_B^-$ $m_B^-$) λ(DE3 [*lacI lacUV5*-T7 gene 1 *ind1 sam7 nin5*]) | EMD Millipore |
| BTH101 | $Sm^R$ | $F^-$, *cya-99 araD139 galE15 galK16 rpsL1* *hsdR2 mcrA1 mcrB1* | (73) |
| MG1655 | | $F^-$, λ$^-$, *rph-1 ilvG$^-$ rfb-50* | (99) |
| MJG1419 | $Cm^R$ | MG1655 Δ*dksA1000*::*cat*$^+$ | (24) |
| MJG1479 | $Cm^R$ | MG1655 Δ*mgtS1000*::*cat*$^+$ | |
| MJG1480 | $Kn^R$ | MG1655 Δ*phoP790*::*kan*$^+$ | |
| MJG1483 | $Kn^R$ | MG1655 Δ*mgtA789*::*kan*$^+$ | |
| MJG1484 | $Kn^R$ | MG1655 Δ*phoQ789*::*kan*$^+$ | |
| MJG1501 | | MG1655 Δ*phoP790* | |

| | | | |
|---|---|---|---|
| MJG1763 | | MG1655 Δ*rpoN730*::*kan*$^{+}$ | (22) |
| MJG1766 | | MG1655 Δ*rpoN730* | (22) |
| MJG1767 | Em$^{D}$ Kn$^{R}$ | MG1655 Δ*rpoE1000*::*kan*$^{+}$ | (22) |
| MJG1955 | Kn$^{R}$ | MG1655 Δ*glrR728*::*kan*$^{+}$ | |
| MJG1956 | Kn$^{R}$ | MG1655 Δ*atoC774*::*kan*$^{+}$ | |
| MJG1969 | Kn$^{R}$ | MG1655 Δ*hyfR739*::*kan*$^{+}$ | |
| MJG1970 | Kn$^{R}$ | MG1655 Δ*pspF739*::*kan*$^{+}$ | |
| MJG1971 | Kn$^{R}$ | MG1655 Δ*norR784*::*kan*$^{+}$ | |
| MJG1972 | Kn$^{R}$ | MG1655 Δ*ygeV720*::*kan*$^{+}$ | |
| MJG1973 | Kn$^{R}$ | MG1655 Δ*rtcR755*::*kan*$^{+}$ | |
| MJG1974 | Kn$^{R}$ | MG1655 Δ*prpR772*::*kan*$^{+}$ | |
| MJG1975 | Kn$^{R}$ | MG1655 Δ*zraR775*::*kan*$^{+}$ | |
| MJG1976 | Kn$^{R}$ | MG1655 Δ*fhlA735*::*kan*$^{+}$ | |
| MJG2058 | Kn$^{R}$ | MG1655 Δ*glnB727*::*kan*$^{+}$ | |
| MJG2061 | Kn$^{R}$ | MG1655 Δ*glnK736*::*kan*$^{+}$ | |
| MJG2064 | Kn$^{R}$ | MG1655 Δ*glnG730*::*kan*$^{+}$ | |
| MJG2065 | | MG1655 Δ*glrR728* | |
| MJG2068 | Kn$^{R}$ | MG1655 Δ*glrR728* Δ*glnG730*::*kan*$^{+}$ | |
| MJG2082 | | MG1655 Δ*glnB727* | |
| MJG2083 | Kn$^{R}$ | MG1655 Δ*glnB727* Δ*glnK736*::*kan*$^{+}$ | |
| MJG2086 | Kn$^{R}$ | MG1655 Δ*ptsN732*::*kan*$^{+}$ | |
| MJG2089 | | MG1655 Δ*ptsN732* | |
| MJG2090 | Kn$^{R}$ | MG1655 Δ*npr-734*::*kan*$^{+}$ | |

| | | |
|---|---|---|
| MJG2091 | $Kn^R$ | MG1655 Δ*ptsP753*::*kan*$^+$ |
| MJG2112 | $Kn^R$ | MG1655 Δ*rapZ733*::*kan*$^+$ |
| MJG2114 | | MG1655 Δ*rapZ733* |
| MJG2151 | $Cm^R$ | MG1655 Δ*glmZ1000*::*cat*$^+$ |
| MJG2155 | $Cm^R$ | MG1655 Δ*glmY1000*::*cat*$^+$ |
| MJG2179 | $Kn^R$ | MG1655 *ptsN*-3xFLAG::*kan*$^+$ |
| MJG2191 | | MG1655 *ptsN*-3xFLAG |
| MJG2193 | $Kn^R$ | MG1655 *ptsN*-3xFLAG Δ*phoP790*::*kan*$^+$ |
| MJG2200 | $Kn^R$ | MG1655 *ptsN*-3xFLAG Δ*rpoN730*::*kan*$^+$ |
| MJG2202 | | MG1655 *ptsN*-3xFLAG Δ*rpoN730* |

Plasmids:

| | | | |
|---|---|---|---|
| pBAD18 | $Ap^R$ | *bla*$^+$ | (58) |
| pBAD24 | $Ap^R$ | *bla*$^+$ | (58) |
| pCDFDuet-1 | $Sp^R$ | *aadA*$^+$ | Novagen |
| pCP20 | $Ap^R$ $Cm^R$ | Flp$^+$ *bla*$^+$ *cat*$^+$ | (101) |
| pDKSA1 | $Ap^R$ | *dksA*$^+$ *bla*$^+$ | (24) |
| pET-21b(+) | $Ap^R$ | *bla*$^+$ | Novagen |
| pGCN4zip1 | $Kn^R$ | T25-*GCN4zip kan*$^+$ | |
| pGCN4zip3 | $Ap^R$ | *GCN4zip*-T18 *bla*$^+$ | |
| pGFP3 | $Sp^R$ | *gfpmut3*$^+$ *aadA*$^+$ | |
| pGFP4 | $Sp^R$ | $P_{mgtS}$-*gfpmut3*$^+$ *aadA*$^+$ | |
| pGLMS1 | $Ap^R$ | *glmS*$^+$ *bla*$^+$ | |
| pGLNB1 | $Ap^R$ | *glnB*$^+$ *bla*$^+$ | |

| | | | |
|---|---|---|---|
| pGLNK1 | $Ap^R$ | *glnK*$^+$ *bla*$^+$ | |
| pKD3 | $Cm^R$ | *cat*$^+$ | (101) |
| pKD46 | $Ap^R$ | λ Red$^+$ *bla*$^+$ | (101) |
| pKNT25 | $Kn^R$ | T25 *kan*$^+$ | (73) |
| pKT25 | $Kn^R$ | T25 *kan*$^+$ | (73) |
| pPPK12 | $Kn^R$ | *ppk*-T25 *kan*$^+$ | |
| pPPK13 | $Kn^R$ | T25-*ppk kan*$^+$ | |
| pPPK33 | $Ap^R$ | *ppk*-GAAEPEA *bla*$^+$ | |
| pPTSN1 | $Ap^R$ | *ptsN*$^+$ *bla*$^+$ | |
| pPTSN2 | $Ap^R$ | *ptsN*$^{C217G, T219A}$ (encoding PtsN$^{H73E}$) *bla*$^+$ | |
| pPTSN3 | $Ap^R$ | *ptsN*$^{C217G, A218C, T219G}$ (encoding PtsN$^{H73A}$) *bla*$^+$ | |
| pPTSN5 | $Ap^R$ | T18-*ptsN bla*$^+$ | |
| pRPOE1 | $Ap^R$ | *rpoE*$^+$ *bla*$^+$ | (22) |
| pRpoN | $Ap^R$ | *rpoN*$^+$ *bla*$^+$ | (103) |
| pSUB11 | $Ap^R$ $Kn^R$ | 3xFLAG *kan*$^+$ *bla*$^+$ | (102) |
| pUT18 | $Ap^R$ | T18 *bla*$^+$ | (73) |
| pUT18C | $Ap^R$ | T18 *bla*$^+$ | (73) |

1016

1017 **TABLE 2.** Primers used for quantitative RT-PCR

| Gene | Forward Primer | Reverse Primer |
|---|---|---|
| *yqfB* | GACGAGTCTGAATCGCACTT | TGTGTCTGACCGGGATAGAT |
| *glmS* | GCAACGTGATGTAGCAGAAATC | CCAGCGAGTGTGAGCAATA |
| *glnK* | GAAGCTGGTGACCGTGATAAT | TCAGCAATCGCCACATCAA |

| | | |
|---|---|---|
| *mgtA* | GGTGATGCCCGAAGAAGAA | CGCCGAGAATGGTGAGTAAA |

## FIGURE LEGENDS

**FIG 1** The bEBPs GlnG and GlrR influence polyP production. (*A*) *E. coli* MG1655 wild-type or Δ*rpoN730* containing either pBAD24 (VOC) or pRpoN (*rpoN*$^+$) plasmids were grown at 37°C to $A_{600}$=0.2–0.4 in LB containing 2 g $l^{-1}$ arabinose (black circles) and then shifted to minimal medium containing 2 g $l^{-1}$ arabinose for 2 hours (white circles)(n=3, ± SD). (*B*) MG1655 wild-type, Δ*glnG730*::*kan*$^+$, Δ*glrR728*, or Δ*glrR728* Δ*glnG730*::*kan*$^+$ were grown at 37°C to $A_{600}$=0.2–0.4 in LB (black circles) and then shifted to minimal medium for 2 hours (white circles)(n=3, ± SD). (*C*) MG1655 wild-type, Δ*rpoN730*, Δ*atoC774*::*kan*$^+$, Δ*hyfR739*::*kan*$^+$, Δ*norR784*::*kan*$^+$, Δ*prpR772*::*kan*$^+$, Δ*pspF739*::*kan*$^+$, Δ*rtcR755*::*kan*$^+$, Δ*ygeV720*::*kan*$^+$, or Δ*zraR775*::*kan*$^+$ were grown at 37°C to $A_{600}$=0.2–0.4 in LB (black circles) and then shifted to minimal medium for 2 hours (white circles)(n=3-6, ± SD). PolyP concentrations are in terms of individual phosphate monomers. Asterisks indicate polyP levels significantly different from those of the wild-type control for a given experiment (two-way repeated measures ANOVA with Holm-Sidak's multiple comparisons test, ** = P<0.01, **** = P<0.0001).

**FIG 2** RpoN-dependent regulation of polyP synthesis is dependent on cellular nitrogen status, but not on GlnB or GlnK *per se*. (*A*) Simplified model of the regulation of GlnA (glutamine synthetase) activity in response to changes in the intracellular glutamate (E) to glutamine (Q) ratio. (*B*) Diagram of the *glnK* and *glnB* loci in *E. coli*. (*C*) *E. coli*

MG1655 wild-type was grown at 37°C to $A_{600}$=0.2–0.4 in rich medium (LB) and then shifted to minimal medium (MOPS with no amino acids, 4 g $l^{-1}$ glucose, 0.1 mM $K_2HPO_4$, 0.1 mM uracil) for 2 hours. qRT-PCR was used to measure fold changes in *glnK* transcript abundance at the indicated timepoints (n=3, ± SD), normalized to expression before stress treatment (t = 0 h). (*D*, *E*) *E. coli* MG1655 wild-type, Δ*rpoN730*, or Δ*dksA1000*::*cat*$^+$ containing either pBAD18 (VOC), pGLNB1 (*glnB*$^+$) or pGLNK1 (*glnK*$^+$) plasmids were grown at 37°C to $A_{600}$=0.2–0.4 in LB containing 2 g $l^{-1}$ arabinose (black circles) and then shifted to minimal medium supplemented with 2 g $l^{-1}$ arabinose for 2 hours (white circles)(n=3-4, ± SD). (*F*) MG1655 wild-type, Δ*dksA1000*::*cat*$^+$, Δ*glnG730*::*kan*$^+$, Δ*glnK736*::*kan*$^+$, Δ*glnB727*, or Δ*glnB727* Δ*glnK736*::*kan*$^+$ were grown at 37°C to $A_{600}$=0.2–0.4 in LBQ (black circles) and then shifted to minimal medium for 2 hours (white circles)(n=3-5, ± SD). PolyP concentrations are in terms of individual phosphate monomers. Asterisks indicate polyP levels significantly different from those of the wild-type control for a given experiment (two-way repeated measures ANOVA with Holm-Sidak's multiple comparisons test, ns = not significant * = P<0.05, ** = P<0.01, **** = P<0.0001). (*G*) *S*pecific activity of purified PPK in the presence of the indicated compounds (n=3, ±SD; one-way ANOVA, ns = not significant).

**FIG 3** Effect of *glmY* and GlmS (glutamine--fructose-6-phosphate aminotransferase) regulation on polyP production. (*A*) Diagram of the GlrR- and PhoP-dependent pathways which regulate GlmS expression in *E. coli*. (*B*) MG1655 wild-type, Δ*phoP790*::*kan*$^+$, Δ*phoQ789*::*kan*$^+$, Δ*mgtA789*::*kan*$^+$, or Δ*mgtS1000*::*cat*$^+$ were grown at 37°C to $A_{600}$=0.2–0.4 in LB (black circles) and then shifted to minimal medium for 2

hours (white circles)(n=3, ± SD). (*C*) *E. coli* MG1655 wild-type was grown at 37°C to $A_{600}$=0.2–0.4 in rich medium (LB) and then shifted to minimal medium (MOPS with no amino acids, 4 g $l^{-1}$ glucose, 0.1 mM $K_2HPO_4$, 0.1 mM uracil) for 2 hours. qRT-PCR was used to measure fold changes in *glmS* transcript abundance at the indicated timepoints (n=3, ± SD), normalized to expression before stress treatment (t = 0 h). (*D*) *S*pecific activity of purified PPK in the presence of the indicated compounds (n=3, ±SD; one-way ANOVA, ns = not significant).

**FIG 4** PolyP regulation by RapZ and GlmS depends on growth conditions. (*A*) *E. coli* MG1655 wild-type, Δ*rapZ733*, Δ*glmZ1000*::*cat*$^+$, or Δ*glmY1000*::*cat*$^+$ were grown at 37°C to $A_{600}$=0.2–0.4 in LB (black circles) and then shifted to minimal medium for 2 hours (white circles)(n=4, ± SD). (*B*) *E. coli* MG1655 wild-type containing plasmids pBAD18 (VOC) or pGLMS1 (*glmS*$^+$) were grown at 37°C to $A_{600}$=0.2–0.4 in LB containing 2 g $l^{-1}$ arabinose (black circles) and then shifted to minimal medium supplemented with 2 g $l^{-1}$ arabinose for 2 hours (white circles)(n=3, ± SD). (*C*) *E. coli* MG1655 wild-type containing plasmids pBAD18 or pGLMS1 were grown at 37°C to $A_{600}$=0.2–0.4 in LB containing 2 g $l^{-1}$ arabinose (black circles) and then shifted to minimal medium containing 4 g $l^{-1}$ arabinose as a sole carbon source for 2 hours (white circles)(n=3, ± SD). (*D*) *E. coli* MG1655 wild-type, Δ*rapZ733*, Δ*glmZ1000*::*cat*$^+$, or Δ*glmY1000*::*cat*$^+$ were grown at 37°C to $A_{600}$=0.2–0.4 in LBQ (black circles) and then shifted to minimal medium containing for 2 hours (white circles)(n=3-4, ± SD). (*E*) *E. coli* MG1655 wild-type containing plasmids pBAD18 or pGLMS1 were grown at 37°C to $A_{600}$=0.2–0.4 in LBQ containing 2 g $l^{-1}$ arabinose (black circles) and then shifted to

1086 minimal medium supplemented with 2 g $l^{-1}$ arabinose for 2 hours (white circles)(n=3, ±
1087 SD). (*F*) *E. coli* MG1655 wild-type was grown at 37°C to $A_{600}$=0.2–0.4 in LB (black
1088 circles) and then shifted to minimal media containing either 4 g $l^{-1}$ glucose, 8 g $l^{-1}$
1089 glycerol, or 4 g $l^{-1}$ glucosamine as sole carbon sources for 2 hours (white circles)(n=3-4,
1090 ± SD). PolyP concentrations are in terms of individual phosphate monomers. Asterisks
1091 indicate polyP levels significantly different from those of the wild-type control for a given
1092 experiment unless otherwise indicated (two-way repeated measures ANOVA with Holm-
1093 Sidak's multiple comparisons test, ns = not significant * = P<0.05, ** = P<0.01, *** =
1094 P<0.001, **** = P<0.0001).
1095
1096 **FIG 5** PtsN positively regulates polyP synthesis regardless of its phosphorylation state
1097 or the presence of glutamine, but does not do so by interacting directly with PPK. (*A*)
1098 Diagram of the nitrogen phosphotransferase system of *E. coli*. (*B,C*) MG1655 wild-type,
1099 Δ*ptsN732*, Δ*npr-734*::*kan*$^{+}$, or Δ*ptsP753*::*kan*$^{+}$ were grown at 37°C to $A_{600}$=0.2–0.4 in LB
1100 (panel A) or LBQ (panel B) (black circles) and then shifted to minimal medium for 2
1101 hours (white circles)(n=3, ± SD). (*D*) MG1655 Δ*ptsN732* containing the indicated
1102 plasmids was grown at 37°C to $A_{600}$=0.2–0.4 in LB containing 2 g $l^{-1}$ arabinose (black
1103 circles) and then shifted to minimal medium supplemented with 2 g $l^{-1}$ arabinose for 2
1104 hours (white circles)(n=3, ± SD). VOC is pBAD18. PolyP concentrations are in terms of
1105 individual phosphate monomers. Asterisks indicate polyP levels significantly different
1106 from those of the wild-type or Δ*ptsN* / VOC control for a given experiment unless
1107 otherwise indicated (two-way repeated measures ANOVA with Holm-Sidak's multiple
1108 comparisons test, ns = not significant * = P<0.05, ** = P<0.01, *** = P<0.001, **** =

P<0.0001). (*E*) *E. coli* BTH101 (*cya*$^-$) containing plasmids expressing the indicated protein fusions were grown overnight in LB and either spotted on LB medium containing 0.5 mM IPTG and 40 µg ml$^{-1}$ X-Gal or lysed for quantitative assay of β-galactosidase activity (n=3, ± SD; ND = not detectable). (*F*) *S*pecific activity of purified PPK in the presence of the indicated compounds (n=3, ±SD; one-way ANOVA, ns = not significant).

**FIG 6** Effect of polyP-inducing nutrient limitation on PtsN levels *in vivo*. *E. coli* MG1655 (*A*) *ptsN*-3xFLAG, (*B*) Δ*phoP790*::*kan*$^+$ *ptsN*-3xFLAG, or (*C*) Δ*rpoN730 ptsN*-3xFLAG strains were grown at 37°C to $A_{600}$=0.2–0.4 in LB and then shifted to minimal medium for 2 hours. At the indicated timepoints, protein samples (n=3, ±SD) were collected and immunoblotted to quantify PtsN-3xFLAG and RecA. Representative blots are shown. Full gels are shown in Supplemental Fig. S3. Asterisks indicate normalized PtsN levels significantly different from those of the wild-type at the indicated timepoint (two-way repeated measures ANOVA with Holm-Sidak's multiple comparisons test, ** = P<0.01).

**FIG 7** PtsN acts downstream of RpoN, upstream of DksA, and independently of RpoE in polyP regulation. MG1655 Δ*ptsN732* (panels *A, B*) Δ*rpoN730* (panel *C*), Δ*dksA1000*::*cat*$^+$ (panel *D*), or Δ*rpoE1000*::*kan*$^+$ (panel *E*) strains containing the indicated plasmids were grown at 37°C to $A_{600}$=0.2–0.4 in LB containing 2 g l$^{-1}$ arabinose (black circles) and then shifted to minimal medium supplemented with 2 g l$^{-1}$ arabinose for 2 hours (white circles)(n=3, ± SD). VOC for panel A is pBAD24 and for panels B-E is pBAD18, and both the LB and minimal medium contained 10 µg ml$^{-1}$

erythromycin for the experiment shown in panel E. PolyP concentrations are in terms of individual phosphate monomers. Asterisks indicate polyP levels significantly different from those of the VOC control for a given experiment (two-way repeated measures ANOVA with Holm-Sidak's multiple comparisons test, ns = not significant * = $P<0.05$, ** = $P<0.01$, *** = $P<0.001$, **** = $P<0.0001$).

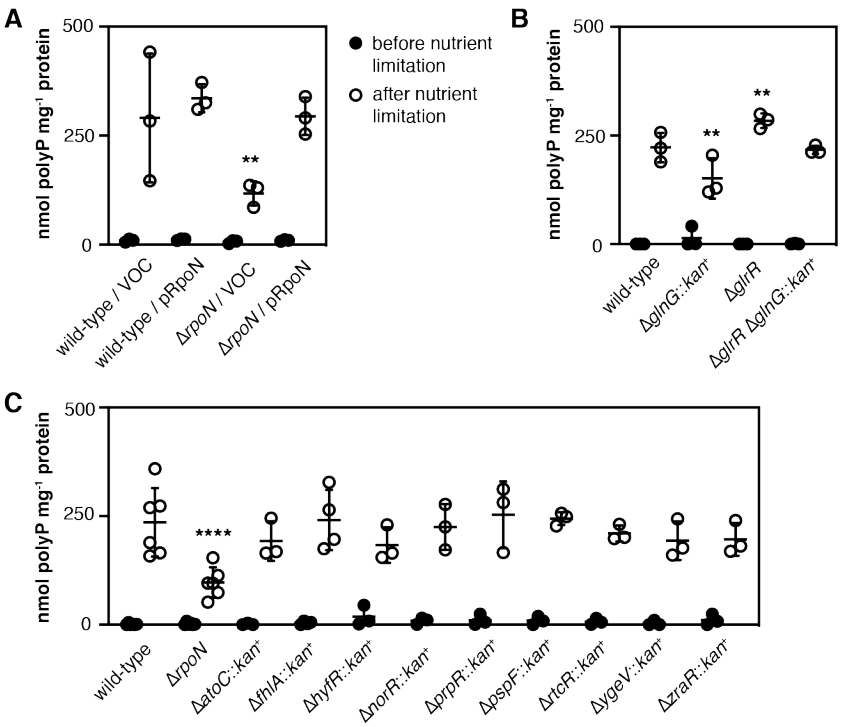


**FIG 1** The bEBPs GlnG and GlrR influence polyP production. (*A*) *E. coli* MG1655 wild-type or Δ*rpoN730* containing either pBAD24 (VOC) or pRpoN (*rpoN*$^+$) plasmids were grown at 37°C to $A_{600}$=0.2–0.4 in LB containing 2 g $l^{-1}$ arabinose (black circles) and then shifted to minimal medium containing 2 g $l^{-1}$ arabinose for 2 hours (white circles)(n=3, ± SD). (*B*) MG1655 wild-type, Δ*glnG730*::*kan*$^+$, Δ*glrR728*, or Δ*glrR728* Δ*glnG730*::*kan*$^+$ were grown at 37°C to $A_{600}$=0.2–0.4 in LB (black circles) and then shifted to minimal medium for 2 hours (white circles)(n=3, ± SD). (*C*) MG1655 wild-type, Δ*rpoN730*, Δ*atoC774*::*kan*$^+$, Δ*hyfR739*::*kan*$^+$, Δ*norR784*::*kan*$^+$, Δ*prpR772*::*kan*$^+$, Δ*pspF739*::*kan*$^+$, Δ*rtcR755*::*kan*$^+$, Δ*ygeV720*::*kan*$^+$, or Δ*zraR775*::*kan*$^+$ were grown at 37°C to $A_{600}$=0.2–0.4 in LB (black circles) and then shifted to minimal medium for 2 hours (white circles)(n=3-6, ± SD). PolyP concentrations are in terms of individual phosphate monomers. Asterisks indicate polyP levels significantly different from those of the wild-

type control for a given experiment (two-way repeated measures ANOVA with Holm-Sidak's multiple comparisons test, ** = P<0.01, **** = P<0.0001).

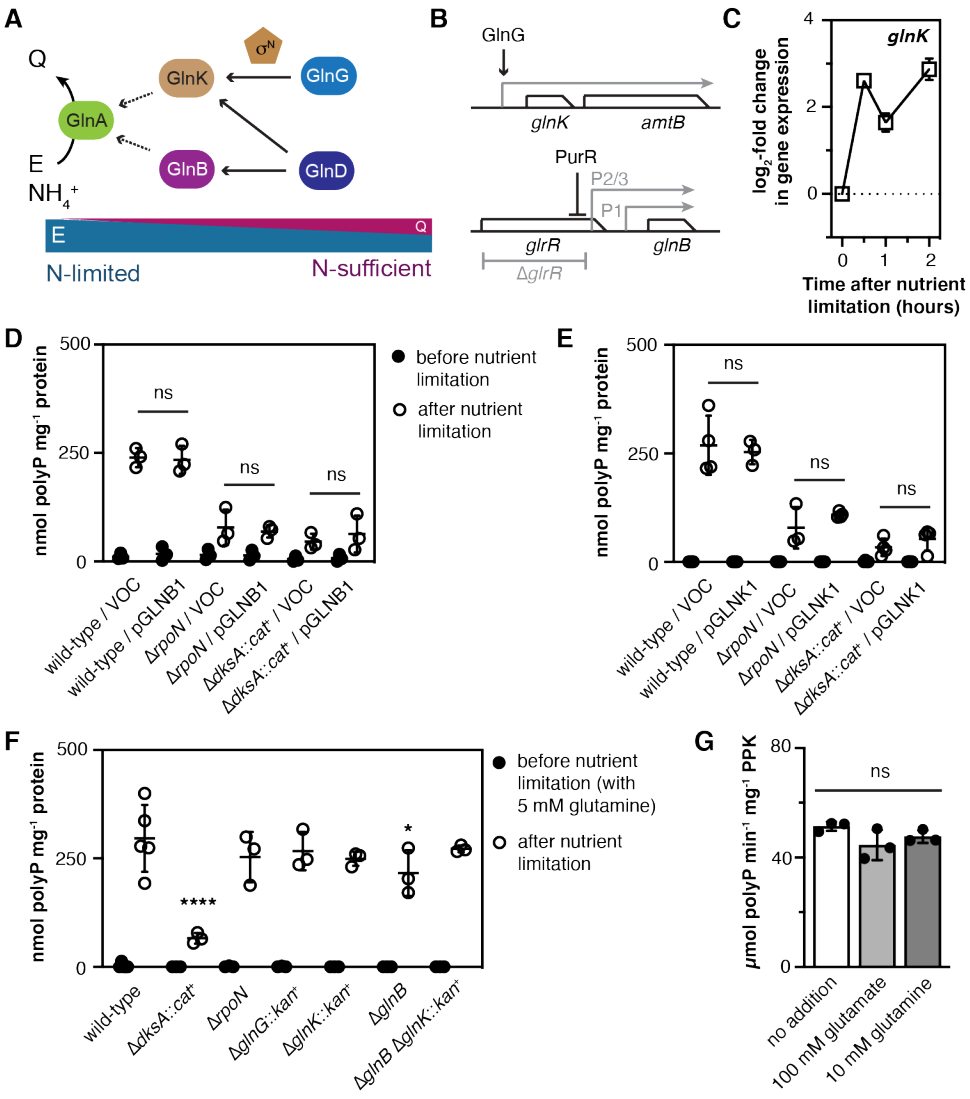


**FIG 2** RpoN-dependent regulation of polyP synthesis is dependent on cellular nitrogen status, but not on GlnB or GlnK *per se*. (*A*) Simplified model of the regulation of GlnA (glutamine synthetase) activity in response to changes in the intracellular glutamate (E) to glutamine (Q) ratio. (*B*) Diagram of the *glnK* and *glnB* loci in *E. coli*. (*C*) *E. coli* MG1655 wild-type was grown at 37°C to $A_{600}$=0.2–0.4 in rich medium (LB) and then shifted to minimal medium (MOPS with no amino acids, 4 g $l^{-1}$ glucose, 0.1 mM $K_2HPO_4$, 0.1 mM uracil) for 2 hours. qRT-PCR was used to measure fold changes in *glnK* transcript abundance at the indicated timepoints (n=3, ± SD), normalized to

expression before stress treatment (t = 0 h). (*D*, *E*) *E. coli* MG1655 wild-type, Δ*rpoN730*, or Δ*dksA1000*::*cat*$^{+}$ containing either pBAD18 (VOC), pGLNB1 (*glnB*$^{+}$) or pGLNK1 (*glnK*$^{+}$) plasmids were grown at 37°C to $A_{600}$=0.2–0.4 in LB containing 2 g $l^{-1}$ arabinose (black circles) and then shifted to minimal medium supplemented with 2 g $l^{-1}$ arabinose for 2 hours (white circles)(n=3-4, ± SD). (*F*) MG1655 wild-type, Δ*dksA1000*::*cat*$^{+}$, Δ*glnG730*::*kan*$^{+}$, Δ*glnK736*::*kan*$^{+}$, Δ*glnB727*, or Δ*glnB727* Δ*glnK736*::*kan*$^{+}$ were grown at 37°C to $A_{600}$=0.2–0.4 in LBQ (black circles) and then shifted to minimal medium for 2 hours (white circles)(n=3-5, ± SD). PolyP concentrations are in terms of individual phosphate monomers. Asterisks indicate polyP levels significantly different from those of the wild-type control for a given experiment (two-way repeated measures ANOVA with Holm-Sidak's multiple comparisons test, ns = not significant * = P<0.05, ** = P<0.01, **** = P<0.0001). (*G*) *S*pecific activity of purified PPK in the presence of the indicated compounds (n=3, ±SD; one-way ANOVA, ns = not significant).

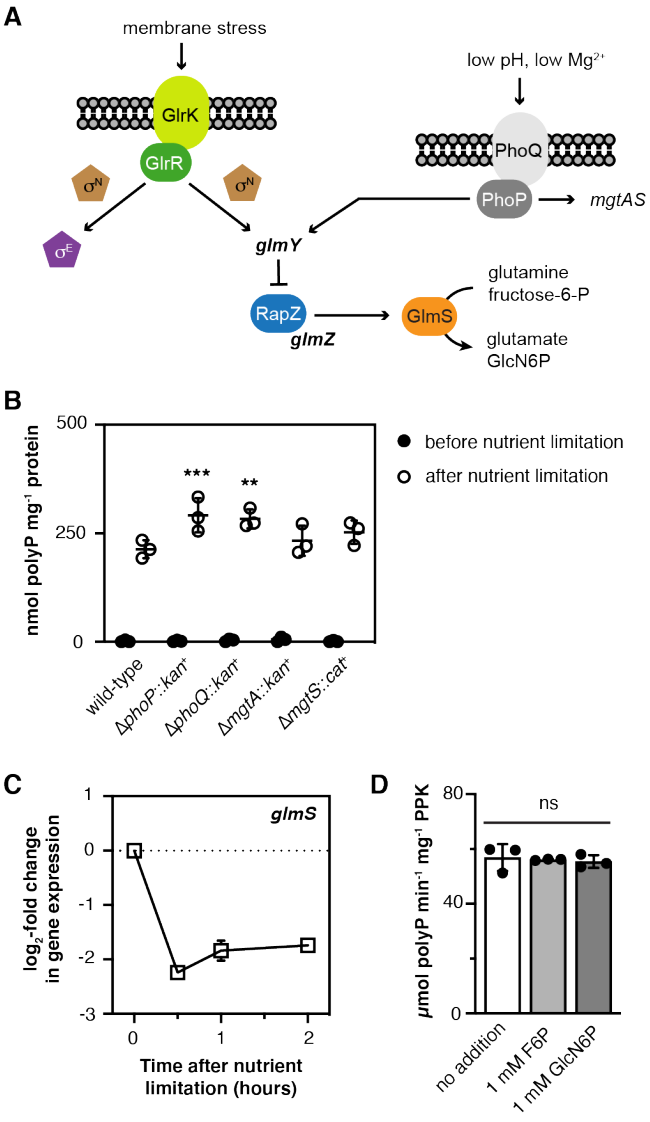


**FIG 3** Effect of *glmY* and GlmS (glutamine--fructose-6-phosphate aminotransferase) regulation on polyP production. (*A*) Diagram of the GlrR- and PhoP-dependent pathways which regulate GlmS expression in *E. coli*. (*B*) MG1655 wild-type, Δ*phoP790*::*kan*$^+$, Δ*phoQ789*::*kan*$^+$, Δ*mgtA789*::*kan*$^+$, or Δ*mgtS1000*::*cat*$^+$ were grown at 37°C to $A_{600}$=0.2–0.4 in LB (black circles) and then shifted to minimal medium for 2 hours (white circles)(n=3, ± SD). (*C*) *E. coli* MG1655 wild-type was grown at 37°C to $A_{600}$=0.2–0.4 in rich medium (LB) and then shifted to minimal medium (MOPS with no amino acids, 4 g $l^{-1}$ glucose, 0.1 mM $K_2HPO_4$, 0.1 mM uracil) for 2 hours. qRT-PCR was

used to measure fold changes in *glmS* transcript abundance at the indicated timepoints (n=3, ± SD), normalized to expression before stress treatment (t = 0 h). (*D*) *S*pecific activity of purified PPK in the presence of the indicated compounds (n=3, ±SD; one-way ANOVA, ns = not significant).

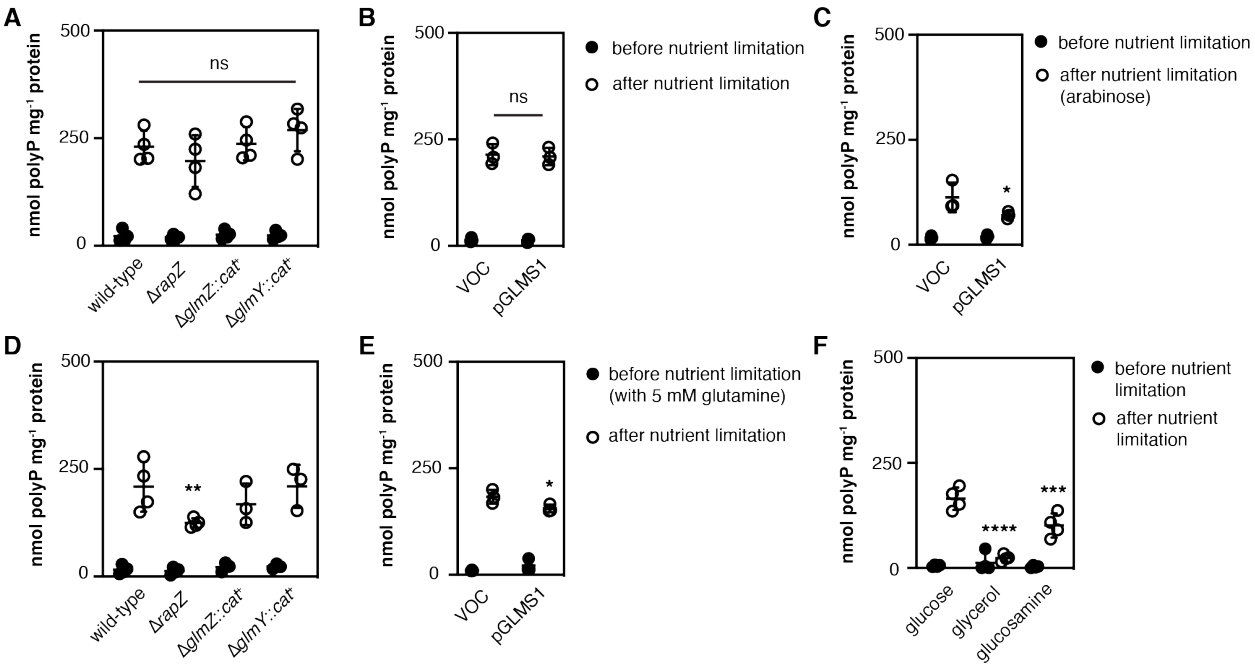


**FIG 4** PolyP regulation by RapZ and GlmS depends on growth conditions. (*A*) *E. coli* MG1655 wild-type, Δ*rapZ733*, Δ*glmZ1000*::*cat*$^+$, or Δ*glmY1000*::*cat*$^+$ were grown at 37°C to $A_{600}$=0.2–0.4 in LB (black circles) and then shifted to minimal medium for 2 hours (white circles)(n=4, ± SD). (*B*) *E. coli* MG1655 wild-type containing plasmids pBAD18 (VOC) or pGLMS1 (*glmS*$^+$) were grown at 37°C to $A_{600}$=0.2–0.4 in LB containing 2 g $l^{-1}$ arabinose (black circles) and then shifted to minimal medium supplemented with 2 g $l^{-1}$ arabinose for 2 hours (white circles)(n=3, ± SD). (*C*) *E. coli* MG1655 wild-type containing plasmids pBAD18 or pGLMS1 were grown at 37°C to $A_{600}$=0.2–0.4 in LB containing 2 g $l^{-1}$ arabinose (black circles) and then shifted to minimal medium containing 4 g $l^{-1}$ arabinose as a sole carbon source for 2 hours (white circles)(n=3, ± SD). (*D*) *E. coli* MG1655 wild-type, Δ*rapZ733*, Δ*glmZ1000*::*cat*$^+$, or Δ*glmY1000*::*cat*$^+$ were grown at 37°C to $A_{600}$=0.2–0.4 in LBQ (black circles) and then shifted to minimal medium containing for 2 hours (white circles)(n=3-4, ± SD). (*E*) *E. coli* MG1655 wild-type containing plasmids pBAD18 or pGLMS1 were grown at 37°C to

$A_{600}$=0.2–0.4 in LBQ containing 2 g $l^{-1}$ arabinose (black circles) and then shifted to minimal medium supplemented with 2 g $l^{-1}$ arabinose for 2 hours (white circles)(n=3, ± SD). (*F*) *E. coli* MG1655 wild-type was grown at 37°C to $A_{600}$=0.2–0.4 in LB (black circles) and then shifted to minimal media containing either 4 g $l^{-1}$ glucose, 8 g $l^{-1}$ glycerol, or 4 g $l^{-1}$ glucosamine as sole carbon sources for 2 hours (white circles)(n=3-4, ± SD). PolyP concentrations are in terms of individual phosphate monomers. Asterisks indicate polyP levels significantly different from those of the wild-type control for a given experiment unless otherwise indicated (two-way repeated measures ANOVA with Holm-Sidak's multiple comparisons test, ns = not significant * = P<0.05, ** = P<0.01, *** = P<0.001, **** = P<0.0001).

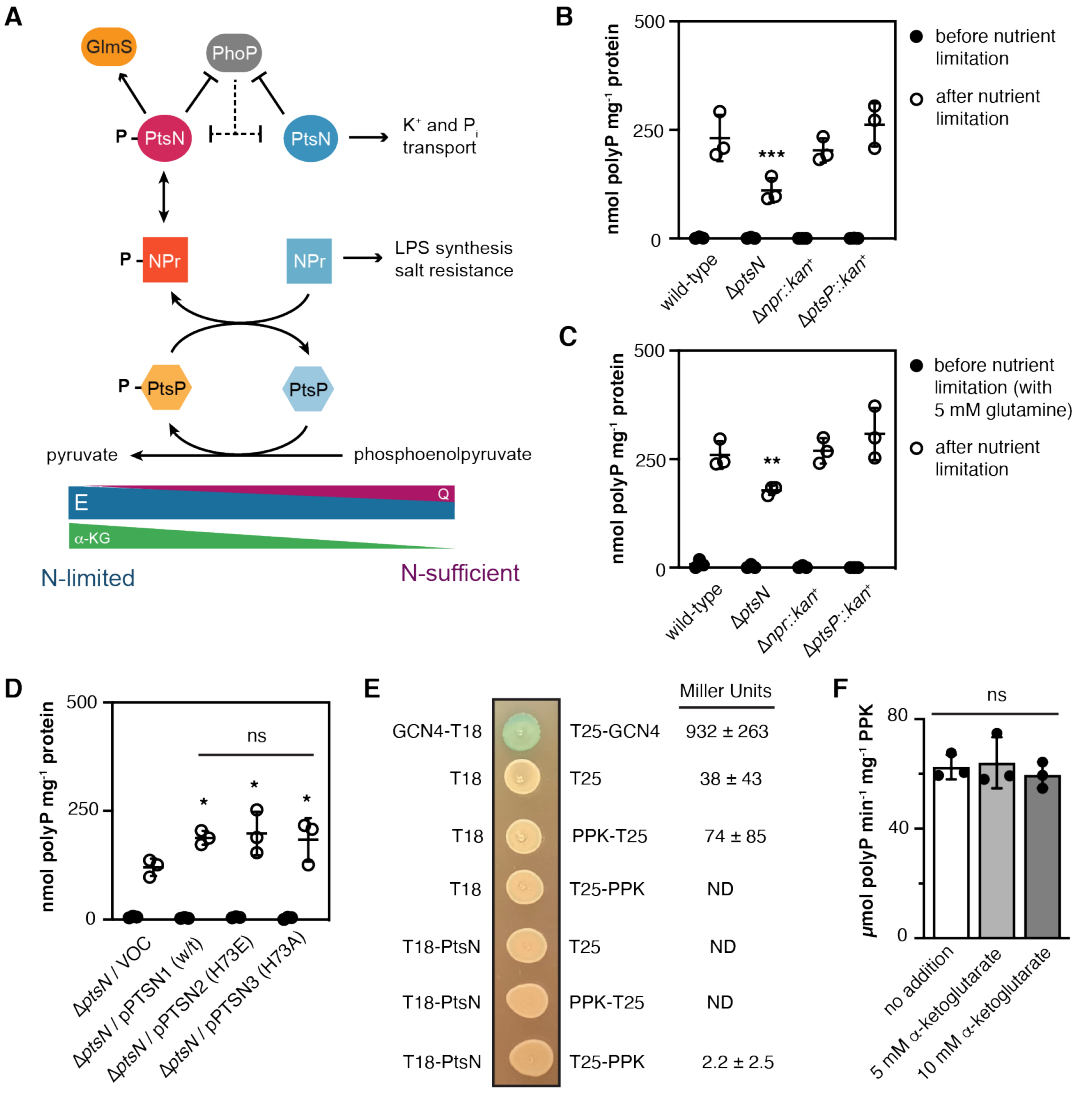


**FIG 5** PtsN positively regulates polyP synthesis regardless of its phosphorylation state or the presence of glutamine, but does not do so by interacting directly with PPK. (*A*) Diagram of the nitrogen phosphotransferase system of *E. coli*. (*B,C*) MG1655 wild-type, Δ*ptsN732*, Δ*npr-734*::*kan*$^+$, or Δ*ptsP753*::*kan*$^+$ were grown at 37°C to $A_{600}$=0.2–0.4 in LB (panel A) or LBQ (panel B) (black circles) and then shifted to minimal medium for 2 hours (white circles)(n=3, ± SD). (*D*) MG1655 Δ*ptsN732* containing the indicated plasmids was grown at 37°C to $A_{600}$=0.2–0.4 in LB containing 2 g $l^{-1}$ arabinose (black circles) and then shifted to minimal medium supplemented with 2 g $l^{-1}$ arabinose for 2

hours (white circles)(n=3, ± SD). VOC is pBAD18. PolyP concentrations are in terms of individual phosphate monomers. Asterisks indicate polyP levels significantly different from those of the wild-type or Δ*ptsN* / VOC control for a given experiment unless otherwise indicated (two-way repeated measures ANOVA with Holm-Sidak's multiple comparisons test, ns = not significant * = P<0.05, ** = P<0.01, *** = P<0.001, **** = P<0.0001). (*E*) *E. coli* BTH101 (*cya*$^-$) containing plasmids expressing the indicated protein fusions were grown overnight in LB and either spotted on LB medium containing 0.5 mM IPTG and 40 μg ml$^{-1}$ X-Gal or lysed for quantitative assay of β-galactosidase activity (n=3, ± SD; ND = not detectable). (*F*) *S*pecific activity of purified PPK in the presence of the indicated compounds (n=3, ±SD; one-way ANOVA, ns = not significant).

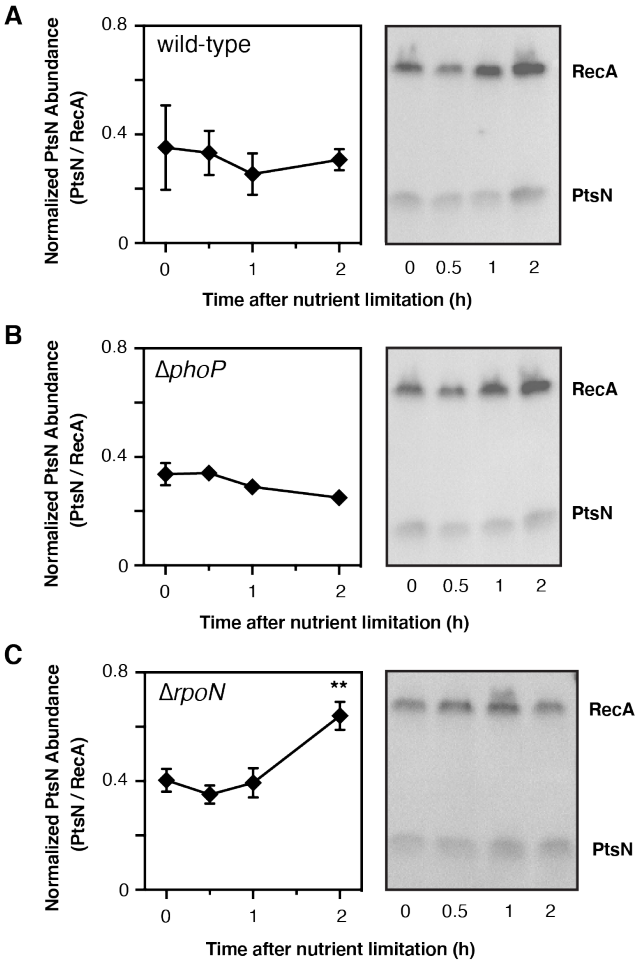


**FIG 6** Effect of polyP-inducing nutrient limitation on PtsN levels *in vivo*. *E. coli* MG1655 (*A*) *ptsN*-3xFLAG, (*B*) Δ*phoP790*::*kan*$^{+}$ *ptsN*-3xFLAG, or (*C*) Δ*rpoN730 ptsN*-3xFLAG strains were grown at 37°C to $A_{600}$=0.2–0.4 in LB and then shifted to minimal medium for 2 hours. At the indicated timepoints, protein samples (n=3, ±SD) were collected and immunoblotted to quantify PtsN-3xFLAG and RecA. Representative blots are shown. Full gels are shown in Supplemental Fig. S3. Asterisks indicate normalized PtsN levels significantly different from those of the wild-type at the indicated timepoint (two-way repeated measures ANOVA with Holm-Sidak's multiple comparisons test, ** = P<0.01).

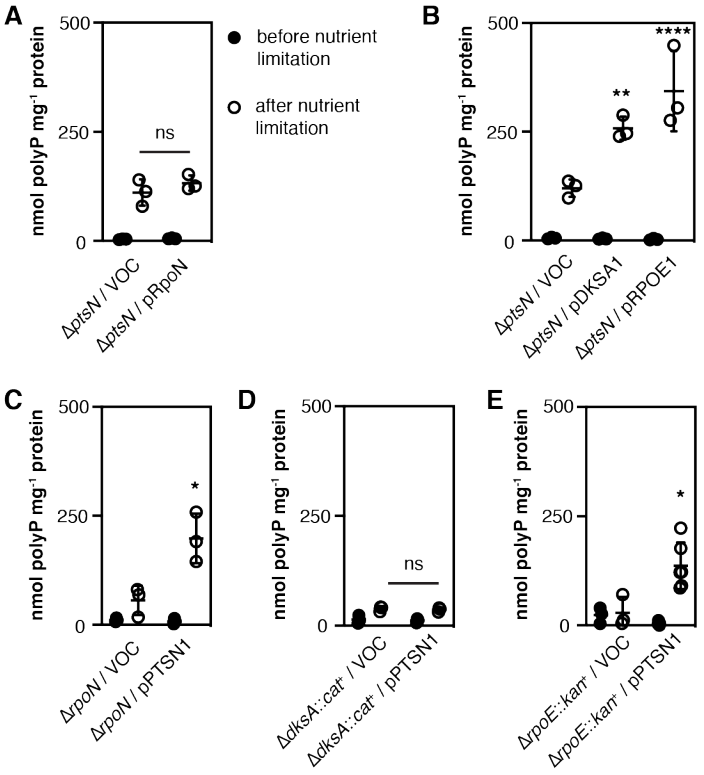


111

112 **FIG 7** PtsN acts downstream of RpoN, upstream of DksA, and independently of RpoE in
113 polyP regulation. MG1655 Δ*ptsN732* (panels *A, B*) Δ*rpoN730* (panel *C*),
114 Δ*dksA1000*::*cat*$^{+}$ (panel *D*), or Δ*rpoE1000*::*kan*$^{+}$ (panel *E*) strains containing the
115 indicated plasmids were grown at 37°C to $A_{600}$=0.2–0.4 in LB containing 2 g $l^{-1}$
116 arabinose (black circles) and then shifted to minimal medium supplemented with 2 g $l^{-1}$
117 arabinose for 2 hours (white circles)(n=3, ± SD). VOC for panel A is pBAD24 and for
118 panels B-E is pBAD18, and both the LB and minimal medium contained 10 μg $ml^{-1}$
119 erythromycin for the experiment shown in panel E. PolyP concentrations are in terms of
120 individual phosphate monomers. Asterisks indicate polyP levels significantly different
121 from those of the VOC control for a given experiment (two-way repeated measures
122 ANOVA with Holm-Sidak's multiple comparisons test, ns = not significant * = P<0.05, **
123 = P<0.01, *** = P<0.001, **** = P<0.0001).